Additive Manufacturing 84 (2024) 104120

Contents lists available at ScienceDirect

Additive Manufacturing

journal homepage: www.elsevier.com/locate/addma

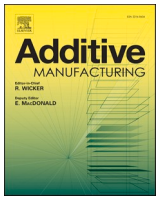

Review

Cyclodextrins in 3D/4D printing for biomedical applications

Carmen Alvarez-Lorenzo *, Alvaro Goyanes, Angel Concheiro

Departamento de Farmacología, Farmacia y Tecnología Farmacéutica, I+D Farma (GI-1645), Facultad de Farmacia, Instituto de Materiales (iMATUS) and Health Research Institute of Santiago de Compostela (IDIS), Universidade de Santiago de Compostela, Santiago de Compostela 15782, Spain

ARTICLE INFO

Keywords:
cyclodextrin
supramolecular assemblies
host-guest interaction
photopolymerization
personalized medicines
wearable sensors

ABSTRACT

Additive manufacturing is one of the key technologies behind recent industrial revolutions. Mass customization requires production techniques that can meet current needs for human-centricity, sustainability, and resiliency. Furthermore, for biomedical applications and personalized medicine, 3D printing demands advanced materials that can respond to the processing requirements of each technique but that are at the same time biocompatible, biofunctional and bioeliminable. Cyclodextrins (CDs) have only recently been explored as components of 3D printed objects despite the variety of functionalities they can offer. Considered safe for most administration routes, these macrocyclic oligosaccharides possess a unique capability to host a wide variety of substances, ranging from small drugs and biomarkers to large peptides and polymers, and can be versatilely functionalized at their numerous hydroxyl groups. Although still underexplored, these capabilities could be transferred to 3D printed structures. The aim of this review is to analyze the contribution of CDs to make 3D/4D printing more sustainable and provide printed objects with novel features. The information collected from the papers published in the last decade has been organized into three sections: CDs to improve drug biopharmaceutical properties and controlled release; CDs as structural agents of 3D printed objects; and CDs as responsive agents for 4D printing and wearable sensors. The obtained results confirm the suitability of CDs to be processed using a variety of 3D printing techniques and to provide new nano-scale tunable architectures, with permanent or stimuli-transient conformations. CDs can expand 3D printing to lipophilic compounds that form inclusion complexes during the preparation of water-based semisolid masses or the melting of filaments or powders. Furthermore, CDs offer several advantages as structural components by forming reversible supramolecular assemblies that exhibit self-healing properties and by facilitating photocross-linking reactions in aqueous environments acting as initiator solubilizer and building blocks. Additionally, CDs can provide 4D behavior through sensitivity to humidity, temperature, pH, ionic strength, and external forces. Overall, CDs can enable 3D printed objects to meet widely varying mechanical, electrical, and drug delivery demands.

1. Introduction

Additive manufacturing is one of the key technologies behind the recent fourth and fifth industrial revolutions. Along the 20th century the industries were able to develop efficient techniques and protocols for production in mass of a variety of objects, which allowed cost reduction and a progressive increase in the quality. As a result of automation, many products, including those related with health and welfare became

Abbreviations: α-CD, alpha-cyclodextrin; β-CD, beta-cyclodextrin; β-CD-Aam, acrylamide-β-cyclodextrin; γ-CD, gamma-cyclodextrin; 2PP, two-photon polymerization; ADME, absorption, distribution, metabolism and excretion; ASC, adipose derived stem cell; BCS, Biopharmaceutical Classification System; BD, 1,3,5-benzenetrialdehyde; BDNF, brain derived neurotrophic factor; CAL, computed axial lithography; CAT, β-carotene; CDs, cyclodextrins; ChCl, choline chloride; CLIP, continuous liquid production interface; CMC, carboxymethylcellulose; CS, chitosan; DLP, digital light processing; DPE, direct powder extrusion; DS, degree of substitution; FFF, fused filament fabrication; HA, hyaluronic acid; HIPE, high internal phase emulsion; HP-β-CD, hydroxypropyl-beta-cyclodextrin; HP-γ-CD, hydroxypropyl-gamma-cyclodextrin; HPC, hydroxypropylcellulose; HPMC, hydroxypropyl methylcellulose; M-β-CD, methyl-beta-cyclodextrin; MAb, monoclonal antibody; PA, peptide amphiphiles; PCL, poly-ε-caprolactone; PEG, polyethylene glycol; PEGMEM, methacrylated polyethylene glycol; PEO, polyethylene oxide; PLA, polylactic acid; PNIPAm, polyN-isopropylacrylamide; PNP, polymer-nanoparticle; PPC, propylene carbonate; PPO, polypropylene oxide; PVA, polyvinyl alcohol; RRAM, resistive random access memory; SCF, simulated colonic fluid; SERS, surface-enhanced Raman spectroscopy; SGF, simulated gastric fluid; SIF, simulated intestinal fluid; SLA, stereolithography; SLS, selective laser sintering; TP:1, 3,5-triformylphloroglucinol; VPP, vat photopolymerization.

* Corresponding author.
E-mail address: carmen.alvarez.lorenzo@usc.es (C. Alvarez-Lorenzo).

https://doi.org/10.1016/j.addma.2024.104120
Received 21 October 2023; Received in revised form 2 April 2024; Accepted 3 April 2024
Available online 5 April 2024

accessible to a broader spectrum of people. However, by the beginning of the 21st century the customers were worried not only on affordability but also on improved performances and personalization. Thus, mass production started to shift to mass personalization or mass customization. This change of paradigm was possible thanks to the advances in both information technologies and operational technologies. "Digitalization" or "physical, digital, and biological convergence" is the main descriptor of Industry 4.0, as "Mechanization", "Electrification", and "Automation" were the driven elements of Industry 1.0 (18th century), Industry 2.0 (19th century), and Industry 3.0 (20th century), respectively. Computerization, digital interconnection of machines, internet of things, the cloud, and advanced engineering, such as additive manufacturing, have fostered the creation of smart factories able to automate the processes further [1].

In less than two decades, the rapid evolution of Industry 4.0 resulted in highly profitable yields of production but at expenses of relevant social metrics, particularly the occupational health of the workers. Driven by new generations of information technologies, the Industry 5.0 aims to "Personalization", i.e., to place the well-being of humans as the main goal of the manufacturing system [2]. In brief, Industry 5.0 reinforces the outcomes of Industry 4.0 through the delivery of highly personalized products and services with an increasing customer empowerment. The Industry 5.0 relies on the combination of artificial intelligence tools and cognitive computing (objective criteria) and the human intelligence, sensitiveness, rationality and creativeness (subjective criteria) to attain an adequate human-robot (cobot) collaboration environment that simultaneously addresses manufacturing and social needs [3]. Thus, the main differential features of Industry 5.0 are human-centricity, sustainability, and resiliency.

In the healthcare field, digitalization has transformed patient care in terms of earlier diagnosis tools, faster identification and development of more precise treatments, and interconnection of health data and patient monitoring with less human effort [4]. Personalization of the automatization, the key feature of Industry 5.0, brings into reality the "personalized" delivery of care for patients. Personalized medicines, medical implants, artificial organs, and transplants adapted to the unique requirements and lifestyle of each patient as well as patient-specific surgical plannings and instruments are now becoming a reality [5,6].

Additive manufacturing, and particularly 3D printing, may strongly contribute to the three pillars of Industry 5.0. Versatile and automatable 3D printing technologies can produce individualized products that perfectly match to each customer needs in a fast and highly reproducible way and that include added value elements for each specific application (human-centricity), using the minimal quantities of raw materials and energy without wastes (sustainability) [7,8]. Moreover, under stress conditions due to natural emergencies, pandemics, border closures, (geo)political conflicts or rapidly changing market conditions, 3D printing technologies offer resiliency (ability to adapt and recover) to the entire manufacturing chain. They also usually lead to lower cost and higher quality products, compared to conventional manufacture technologies, that can be accessible to more people and that can be produced where they are needed (e.g., at a point of care) by sending or sharing through internet the adequate files, avoiding the costs of transport of the final products [9,10].

In the health care field, 3D printing technologies help overcoming the constrains of "one-size-fits-all" medicines by providing patient-adapted products [11,12]. 3D printing has already allowed for the personalization of doses and excipients in medicines produced in hospital setups [13], preparation of customized models and tools for more efficient surgeries [14,15], cost-effective design of high-quality personalized implants with an extended self-life period [16–18], or orthopedic implants with smart sensors built into them for real-time monitoring of implant performance and patient outcomes [19].

Although still at the research level, the evolution of 3D printing to 4D printing allows for the production of objects with properties that evolve along time to better fit to physiological environments [20]. More recently, non-planner slicing and printing allow producing curved layers, instead of depositing flat layers, by moving the print part, which results in continuous and stronger curved surfaces and more robust final objects [21]. Such a technology may notably expand the use of additive manufacturing to produce implantable medical devices that have complex curved surfaces, as it is the case of bone scaffolds, without the need of sacrificial materials during printing and exhibiting improved mechanical behavior [22].

To fulfil the Industry 5.0 principles, the innovations in cutting-edge 3D/4D printing technologies should come together with advanced materials and sustainability. On one hand, improved performances of the medicines and medical devices do not depend only on the design but also on the materials they are made of. Bioactive materials able to regulate specific biofunctions (e.g., inhibition of drug efflux pumps in the case of a medicine, or promotion of cell differentiation in the case of a scaffold) are demanded. In same cases there is a mismatch between the materials that are suitable for a printing technology, which are commonly synthetic monomers and polymers, and the biocompatibility and clearance requirements. Absence of safety data causes a delay in the (pre)clinical testing of the novel printed medicines and devices. On the other hand, the use of synthetic monomers and polymers, which are in most cases derivatives of petroleum, raises concerns on sustainability and environmental impact. The accumulation of plastic-like disposable medical devices (a typical example is contact lenses), devices that must be replaced periodically (e.g., catheters), or patient-specific surgical models that are discarded after healing can have a very negative impact on the environment [23,24]. Regulatory agencies are concerned on how non-biodegradable medical devices could be reprocessed to be reused [25]. In this line, 3D printing technologies should be ideally moved to "green" materials [26]. Overall, innovation in materials science and development of multimaterial printing strategies have been identified as two urgent needs of additive manufacturing for biomedical applications [17,27].

Natural polysaccharides, especially cellulose derivatives, are gaining increasing attention as components of 3D printed materials. Microcrystalline cellulose and cellulose ethers and esters are recognized as safe excipients of medicines since many decades ago. Moreover, they are useful as components of medical devices endowed with a variety of functionalities [28]. Cellulose derivatives have recently been shown to be suitable for fused filament fabrication (FFF) and extrusion (bio) printing if their particle size, molecular weight, crystallinity and degree of substitution are adequately tunned [29–32].

Cyclodextrins (CDs) have been much less explored despite the variety of additional functionalities that they may offer. Natural α-CD, β-CD and γ-CD are made of six, seven and eight glucopyranose units, respectively, connected by α-1,4-glycosidic bonds forming a truncated cone-like structure (Fig. 1**A**) [33]. These macrocyclic oligosaccharides are obtained from enzymatic degradation of starch [34]. Differently to the linear or branched polysaccharides, the peculiar cyclic structure of CDs endows these oligosaccharides with the capability to host a wide variety of substances forming inclusion complexes (Fig. 1**B**). CDs have been demonstrated to be safe solubilizing agents of Biopharmaceutics Classification System (BCS) Class II and Class IV drugs in a variety of already approved medicines [35]. Such hosting capability may solve some critical problems of the extrusion 3D printing of hydrophobic drugs in aqueous environment and FFF 3D printing of labile biological active ingredients, avoiding phase separation and providing stability during processing. CDs can regulate the release of the active ingredients through affinity driven mechanisms but also serving as structural agents that reinforce the mechanical properties of the printed objects [36,37]. Host-guest interactions formed with polymeric components may confer (bio)inks with outstanding viscoelastic and self-supportive properties for fast and high-fidelity 3D printing under mild stress conditions (Fig. 1**C**) [38,39]. Moreover, CDs can be easily functionalized with polymerizable moieties to obtain photopolymerizable bio(inks) [40]. In

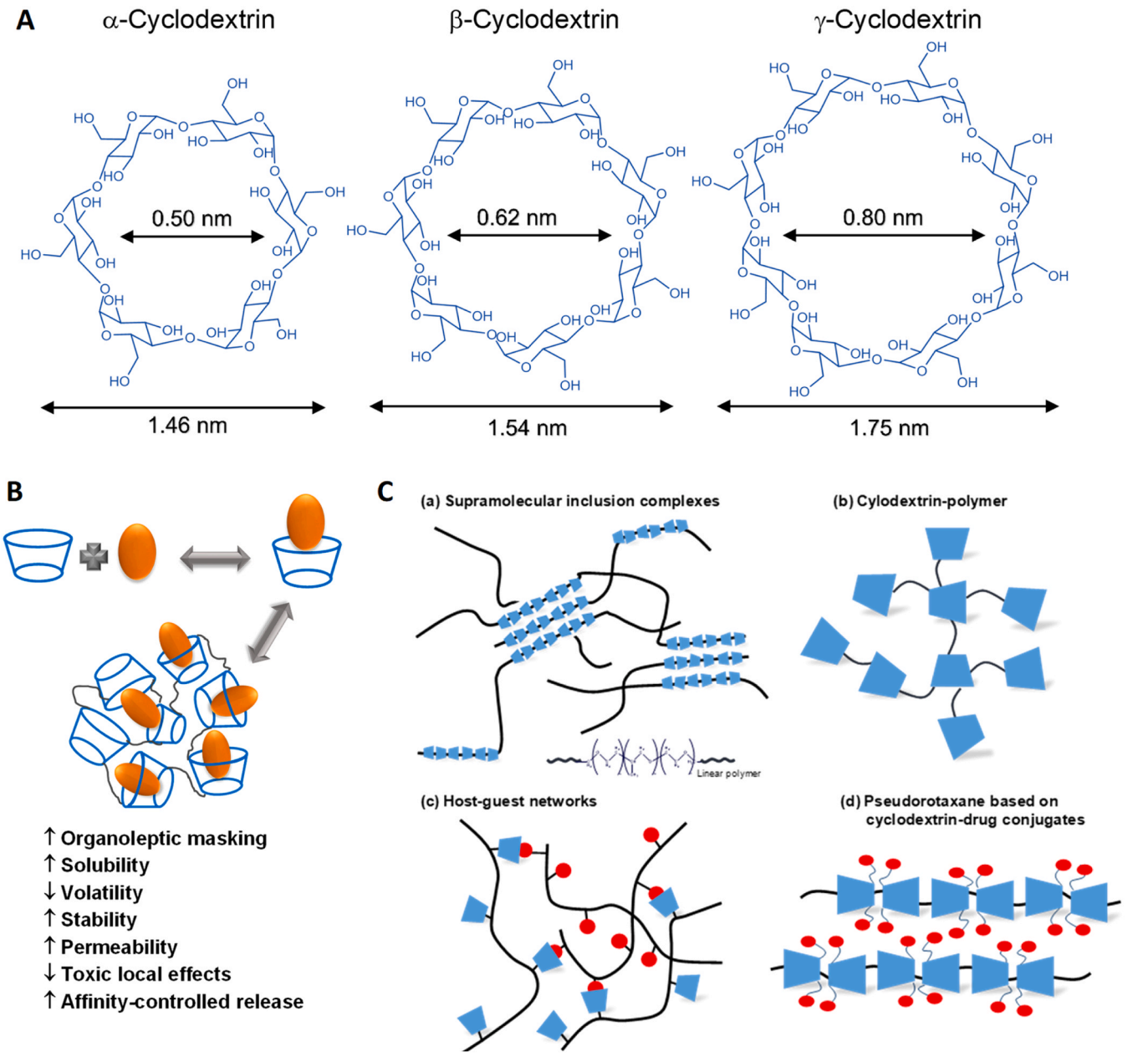

Fig. 1. (A) Structure and approximate inner diameter and outer diameter of α-CD, β-CD and γ-CD; the heigh of all of them has been estimated to be 0.78 nm. Data taken from Loftsson and Brewster [33]. (B) Cyclodextrins can form reversible inclusion complexes with a variety of drugs, resulting in masking of unpleasant organoleptic properties, enhanced drug solubility, stability and permeability, and decreased volatility and toxic local effects. The inclusion complexes can self-aggregate or can be cross-linked resulting in affinity-driven drug-controlled release systems. (C) Cyclodextrin can also (a) be threaded by polymers forming poly (pseudo)rotaxanes that self-assemble as supramolecular structures, (b) be cross-linked forming cyclodextrin-polymers, (c) be grafted to polymers and then form supramolecular architectures through host-guest interactions with polymers functionalized with suitable guests, resulting in zipper-like assemblies, and (d) participate simultaneously in inclusion complexes with drugs and polymers, which may assemble in supramolecular architectures. Reproduced from Simoes et al. [37] with permission from the Royal Society of Chemistry.

addition to the role as excipient and structural agent, CDs can also develop certain "pharmacological" functionalities [41]. For example, they can tune the differentiation of mesenchymal stem cells to chondrocytes, adipocytes or osteoblasts [42,43], or can act as traps of a variety of physiological substances, biomarkers and even *Quorum Sensing* signaling molecules, interfering with biofilm development and synergistically promoting the antimicrobial activity of antibiotics [44,45]. This trap-like functionality can be extended to other fields of applications, such as bioremediation, selective extraction of phytochemicals and nutrients [46], substrates for surface-enhanced Raman spectroscopy (SERS) sensors [47] or surfaces for specific molecular recognition (molecular print boards) [48]. Although still little explored, these capabilities could be transferred to 3D printed structures.

A search in the Web of Science database (updated in February 2024) for the "cyclodextrin AND 3D print*" term provided 68 articles and 9 reviews published until December 31, 2023 (Fig. 2). The topic has been intensified in the last five years. Further analysis of the reviews revealed that they were general reviews on supramolecular assemblies including also assemblies in which CDs were not involved (six contributions), sponges (one), medical devices containing CDs but not focused on 3D printing (one), and 3D printed devices in which cyclodextrins are referred in the Keyword Plus but not tackled among the contents (one).

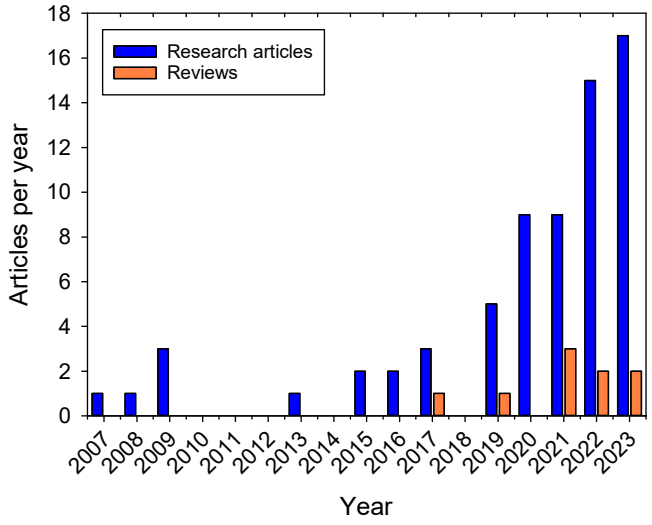

Fig. 2. Outcomes of searching for "cyclodextrin AND 3D print*" term in the Web of Science database until December 2023 (included).

Therefore, a review on the role that CDs may play in 3D/4D printing of medicines and medical devices is missed. The aim of the present review is to fill this gap through a detailed analysis of the available original research papers in order to shed light on the contribution of CDs to make 3D/4D printing more sustainable while endow the printed objects with novel performances. The information has been divided in three sections according to the CD main function disregarding the 3D printing technology applied. These sections comprise: CDs to improve drug biopharmaceutical properties and controlled release; CDs as structural agents of 3D printed objects; and CDs as responsive agents for 4D printing and wearable sensors. The ultimate goal is for the information to be useful for producing personalized devices that exhibit new capabilities or functionalities while meeting the highest standards of safety, biodegradability and sustainability.

2. CDs to improve drug biopharmaceutical properties and to tune drug release

Development of personalized medicines demands not only the discovery of the most adequate drug for each patient but also the preparation of the most adequate dosage form or delivery system for a given drug-patient pair. Careful selection of the dose, the excipients, the morphology of the dosage form, and the drug release place and rate may make medicines to be safer and more efficient. Relevant phenotypic differences in absorption, distribution, metabolism and excretion (ADME) strongly determine the response of the patients to a given treatment. These differences can also be dependent on the age, gender, and health and societal conditions of the patient [49]. 3D printing, mainly FFF and extrusion techniques, has revealed as a very versatile tool to prepare personalized medicines [50]. Printlets is an acronym used to design tablet-like formulations obtained by 3D printing. Preparation of chewable printlets for children suffering from rare metabolic diseases in a hospital setting has already represented a first milestone [13]. Since most drugs are either poorly water soluble or present stability problems, incorporation of CDs may help overcoming these problems and notably expand the functionalities of the oral printlets.

2.1. Extrusion 3D printing

Very hydrophobic drugs, such as carbamazepine (BCS Class II), have been formulated as fast dissolving (in mouth) printlets with the aid of HP-β-CD [51]. Carbamazepine is an antiepileptic and anticonvulsant drug used for the treatment of seizure disorders and neuropathic pain [52]. This drug readily formed inclusion complexes with HP-β-CD during the preparation of a mass suitable for 3D micro-extrusion. A high fix proportion of drug (24% w/w) was blended with HP-β-CD (72.1% w/w; Kleptose® HP oral grade) in a mortar. Then, hydroxypropyl methylcellulose (HPMC) F4M:croscarmellose sodium (Ac-Di-Sol® SD711) 1.4:2.5% w/w mixture (formulation I) or HPMC F4M solely (3.9%) (formulation II) was added as wet gels (water:ethanol 90:10 vol/vol) to the mortar for further blending. The obtained wet masses had viscoelastic and self-healing properties adequate for direct extrusion. Cylindrical printlets (15 mm diameter x 3 mm height) were designed with diagonal (45°) infill pattern and 1 mm pore size and 5 layers (Fig. 3 **A1**). The printlets were dried at 40 °C for 12 h. Formulation I performed as orodispersible (flash; disintegration in 3 min) while formulation II was characterized as of immediate release (disintegration in 7.5 min). The chosen drug:HP-β-CD mass ratio allowed for inclusion complex of half the drug dose as verified by differential scanning calorimetry (DSC) and XRD analysis. The amorphization of a large proportion of carbamazepine and the high hydrophilicity of HP-β-CD explained the fast disintegration of the printlets and the release of the drug; namely, in 15 min formulation I released more than 95% dose and formulation II released 55% dose (Fig. 3 **A2**). Overall, this first report on HP-β-CD as main component of extrusion 3D printed formulations revealed the feasibility of producing oral printlets for patients that require rapid drug release under emergence conditions and with compromised swallowing capability. Only very small proportions of other cellulose derivatives were needed to produce a printable mass, and tiny changes in the ratio of hydrophilic (HPMC) to swellable (croscarmellose sodium) cellulose ethers allowed a fine tuning of the wet masses rheology, which in turn determined printability, the printlets disintegration, and the drug release rate.

β-Cyclodextrin (β-CD) has been shown critical for the efficient encapsulation of the lipophilic β-carotene in wet masses also containing chitosan for extrusion 3D printing [53]. The ink containing β-CD remained stable for 5 days at 25 ºC, compared to the ink lacking inclusion complex formation that was instable. The order of addition of the components, first cyclodextrin and then chitosan, was demonstrated as critical for the correct stabilization of the inclusion complexes (Fig. 3 **B1**) and the long-term stability of the inks. The total content in chitosan determined the rheological properties of the ink (Fig. 3 **B2**) The ink was successfully tested for decoration of bread and paper (Fig. 3 **B3-B7**). Replacing β-carotene with other lipophilic nutrients or supplements the ink might be suitable for nutraceutical products [54].

Semi-solid extrusion 3D printing of inclusion complexes has also been explored for oral administration of cannabidiol. This drug has a plethora of properties ranging from anti-inflammatory to neuroprotective, without psychoactive effects. Cannabidiol is poorly soluble in water and suffers from an extensive first-pass effect in liver; therefore, formulations that specifically release the drug in colon are needed. Pectin from citrus peel (gelling agent) and Manuka honey (adjuvant of gelling) were chosen as natural structural components of the ink. Solid inclusion complexes of cannabidiol and β-CD (1:14 w/w) were added to the pectin:honey (13:2 mass ratio) up to a final concentration of 1%, 2% and 5% w/w [55]. The inclusion complexes facilitated the homogeneous dispersion of the drug in the 3D printed films (1 cm diameter, 0.2 mm thickness). In vitro release tests revealed that the films did not release cannabidiol in simulated gastric fluid and that the release rate was slow in simulated intestinal fluid. Once in contact with simulated colonic fluid, a burst release occurred (Fig. 3 **C**). The total content in inclusion complexes caused minor changes in the release pattern, but films prepared with 2% and 5% inclusion complexes provided more reproducible release data compared to 1%, probably because a more homogeneous distribution of the drug in the films.

High methoxylated pectin and Manuka honey mixtures were also used for the 3D printing of wound dressings due to excellent sorption of exudates and antimicrobial activity. Incorporation of propolis, with diverse potential therapeutic activities, was investigated in the form of

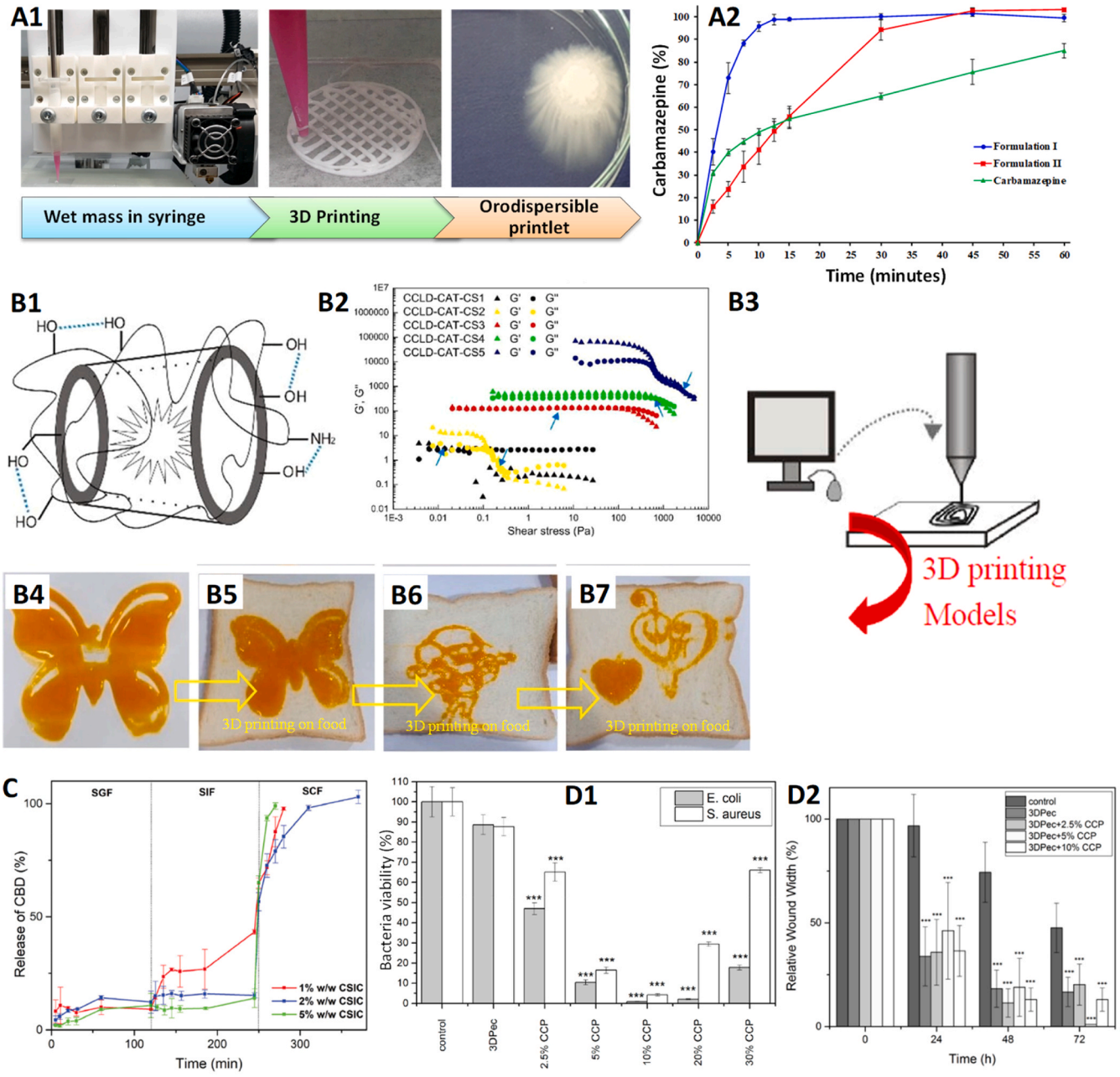

Fig. 3. (A1) Printlets of carbamazepine were prepared by extrusion 3D printing using as main component HP-β-CD. The wet mases had adequate printability performance, showed fast disintegration in contact with aqueous medium and (A2) accelerated drug dissolution compared to the same mass of free drug as crystalline powder. Reproduced from Conceição et al. [51] with permission from Elsevier. (B1) Inclusion complexes of β-carotene (CAT) with β-cyclodextrin (CCLD) were stabilized with chitosan (CS); (B2) increasing the content of chitosan in the wet mass, the values of storage (G') and loss (G'') moduli also increased, with the most favorable mechanical properties observed for CCLD-CAT-CS4 (CCLD solution: CAT: CS solution =50:2:50) (values in green); and (B3) the wet mass was 3D printed (extrusion) with a nozzle of 1 mm diameter at 30 ºC on (B4) paper and (B5-B7) bread and the pictures taken one hour after. Reproduced from Wang et al. [53] with permission from Elsevier. (C) Effect of pH on cannabidiol release from 3D printed pectin-honey films prepared with 1%, 2% and 5% solid inclusion complexes of cannabidiol:β-cyclodextrin (CSIC) and tested in simulated gastric fluid (SGF), simulated intestinal fluid (SIF), and simulated colonic fluid (SCF). Reproduced from Andriotis et al. [55] with permission from Taylor & Francis. (D) Antimicrobial activity (D1) and wound healing properties (D2) of 3D-printed pectin:honey films containing 0%, 2.5%, 5%, 10%, 20% and 30% w/w chitosan-β-cyclodextrin-propolis (CCP) inclusion complexes; *** $p < 0.05$ vs. control. Adapted from Andriotis et al. [56] (Creative Commons Attribution (CC BY) license).

inclusion complexes with β-CD that were combined with chitosan (designed as CCP) [56]. The patches were 3D printed covering a wide range of chitosan-containing inclusion complexes (0%, 2.5%, 5%, 10%, 20% and 30% w/w CCP with respect to dry pectin). As the content in inclusion complexes increased, the film structure became more heterogeneous and the disintegration time increased due to the ionic cross-linking of chitosan with pectin. An adequate balance between film physical properties, antimicrobial activity and wound healing was found for a 10% CCP (Fig. 3 **D1-D2**).

The capability of β-CD to form inclusion complexes with essential oils exhibiting antimicrobial properties is also being exploited to develop 3D printed active packaging of fruits. Inclusion complexes of β-CD and lemongrass essential oil mixed with sodium alginate have been suitable for strawberry preservation [57].

2.2. Fused Filament Fabrication 3D printing

FFF 3D printing requires the previous preparation of a filament containing all components by means of hot-melt extrusion. Thus, the FFF technique involves two successive melting-cooling steps; namely, one to prepare the filament and a second one for 3D printing. Hot-melt extrusion has been widely shown as an efficient technique to form CD-based inclusion complexes in a continuous production mode and also including adjuvant polymers [58,59]. Thus, FFF 3D printing appears as a suitable technique to develop the encapsulation potential of cyclodextrins.

HP-β-CD has been tested as stabilizing agent of a monoclonal antibody (mAb) during hot melt extrusion and subsequent FFF. However, the proportion of HP-β-CD used was quite low (3.2–5.1%), and trehalose associated to isoleucine showed better stabilization properties. Thus, the study was not further progressed with HP-β-CD [60].

Recently, paclitaxel and carboplatin were formulated as drug-eluting intrauterine implants by combining poly-ε-caprolactone (PCL; Mn 80,000) and cyclodextrins [61]. These drugs are poorly soluble in water and their dose ratio is different for each patient. Therefore, there is the two-fold need of preparing personalized devices and improving drug solubility. HP-β-CD, methyl-β-cyclodextrin (M-β-CD), and hydroxypropyl-γ-cyclodextrin (HP-γ-CD) were tested. The inclusion complexes were prepared by a co-precipitation method and those prepared with a drug:M-β-CD 1:1 molar ratio showed the highest encapsulation efficiency for both paclitaxel and carboplatin. Filaments (1.75 mm diameter) were prepared with each inclusion complex in separate by heating in the 75–80 ºC range; final paclitaxel:PCL ratio was 1:1000 w/w and carboplatin:PCL ratio was 1:2000 w/w. Carboplatin:M-β-CD filaments showed faster release than paclitaxel:M-β-CD filaments, but in any case, the release was sustained for several days. The higher release rate of carboplatin:M-β-CD filaments was ascribed to the higher intrinsic solubility of carboplatin and its inclusion complexes compared to paclitaxel, which in turn facilitates the migration of the drug towards the filament surface. The obtained release rates were adequate for causing the death of HEC-1B human endometrial adenocarcinoma cells.

In the field of regenerative medicine, β-CD has been added to 3D printed polylactic acid (PLA)-based scaffolds to provide sustained delivery of antimicrobial agents, avoiding initial burst release. β-CD: chlorhexidine 1:1 inclusion complexes were mixed with PLA and nanohydroxyapatite (nHA) in a mass ratio of 3:80:20 and printed at 105 ºC [62]. Compared to scaffolds lacking inclusion complexes, those prepared with β-CD:chlorhexidine efficiently prevented microorganisms colonization while showing excellent compatibility with osteoblast precursor cell line and bone formation in cell cultures.

2.3. Direct powder extrusion (DPE) 3D printing

HP-β-CD has been shown also suitable for direct powder extrusion (DPE) 3D printing. This technique avoids the previous preparation of a filament, as required for FFF, which shortens the production process.

In a first report, this printing technique was applied to overcome the poor oral bioavailability of niclosamide, which is a BCS Class II antihelmintic repositioned for the treatment of tumors. Direct powder extrusion (DPE) 3D printing of mixtures of the drug (10% w/w) with HPMC Affinisol™ 15LV (42.87–40.73% w/w), HP-β-CD (Cavasol W7) (47.13% w/w) and polyethylene glycol (PEG) 6000 (2.14–4.50% w/w) was shown to notably increase niclosamide dissolution rate (100% release in 24 h) compared to formulations lacking HP-β-CD (65–70% release in 48 h). During the extrusion through the nozzle (0.8 mm) at 180 ºC, the drug was amorphized and blended with the excipients, facilitating the inclusion complex formation. The obtained printlets (12 mm diameter x 3.7 mm height) had homogeneous content in drug and close to the feeding values [63].

DPE 3D printing was shown also suitable for improving the oral solubility of budesonide (BCS Class II) intended for the treatment of eosinophilic colitis in pediatric patients [64]. Mini-tablets (5 mm diameter x 4 mm thickness) were prepared to perfectly adjust the dose and to facilitate the swallowing. Budesonide proportion was fixed at 0.59% w/w and tested either as (i) a physical mixture with HPMC 15LV (75.44%):PEG 6000 (3.97%) (named MT1), (ii) a physical mixture with HPMC 15LV (41.84%):PEG 6000 (2.99%):HP-β-CD (46.41%) (named MT2), or (iii) inclusion complexes of budesonide and HP-β-CD previously prepared by freeze-drying (47.00%) mixed with HPMC 15LV (41.84%):PEG 6000 (2.99%) (named MT3). The printlets were prepared through a nozzle of 0.4 mm at 180 ºC, except for the inclusion complexes, which required 190 ºC, due to the worsening of the powder flow properties (Fig. 4 **A1**). Compared to free budesonide powder that dissolved only up to 14% in pH 7.4, mini-tablets prepared with HP-β-CD exhibited a rapid drug release under all pH conditions (100% released in 10 h) (Fig. 4 **A2**). The results evidenced that the previous preparation of inclusion complexes is not needed, and they are formed during the one-step mixing and extrusion process inside the printer. Coating with Eudragit FS 30D for the site-specific release at colon allowed preventing drug release at gastric (pH 1.2) and small intestine (pH 6.8) conditions, while the release was triggered at colon conditions (pH 7.4) [64]. Recently, mucoadhesive orodispersible films containing clobetasol propionate have been developed using a similar DPE 3D printing approach for personalized pediatric therapies [65].

2.4. Inkjet printing

Cyclodextrins are particularly suitable as solubilizing agents in inks to be used in inkjet printing. Paclitaxel:HP-β-CD 1:2 molar ratio inclusion complexes prepared by co-lyophilization were dispersed in water: propylene glycol 40:60 v/v mixture and printed onto hydroxypropylcellulose (HPC Klucel LF) films (Fig. 4 **B1**) [66]. The printed films were tested *ex vivo* in a dynamic simulated cervix environment, and the amount of paclitaxel retained in the tissue quantified (Fig. 4 **B2**). The film containing approx. 1 μg paclitaxel was placed in contact with the tissue and simulated vaginal fluid was added dropwise on the cervix tissue at a rate of 5 mL/h. The fluid lacking from the tissue was collected at specific time intervals (15, 30 min, and 1, 2, 6, 16 h). A burst of paclitaxel release (50%) occurred in the first 30 min, and then the delivery was sustained for 16 h (Fig. 4 **B3**). This release pattern was related to the fast dissolution of the inclusion complexes located at the surface of the film, while the bulk of the film acted as a reservoir. Subsequent studies demonstrated that the printed films maintained the anticancer activity of the drug [67].

2.5. Selective laser sintering

Selective laser sintering (SLS) involves the use of a laser for the surface binding of powder particles. The technique starts with the sintering of the particles in a layer, then this layer moves down, more powder particles are deposited on the top, and a new laser irradiation is applied on the particles. SLS causes the agglomeration of the particles according to a predefined 3D pattern. Then, the non-used particles are removed [68]. The powder aggregation resembles the traditional granulation process well implanted in the pharmaceutical industry, but using lasers able to slightly melt the surface of the particles instead of applying a binder solution. The obtained 3D medicine can be made to have high internal porosity, which facilitates a rapid disintegration once in contact with the physiological fluids. SLS is still timidly explored for drug formulation.

CDs can play the two-fold role of increasing drug dissolution rate and also of masking unpleasant taste. Ondasetron is an anti-emetic drug that requires a precise dosing because of its relevant cardiac side effects. Dose personalization has been explored using SLS while using inclusion complexes with β-CD [69]. Two formulations were prepared with a fix content in inclusion complex (22% w/w) and Candurin® Gold Sheen (3% w/w), which served as a yellow colorant that increases the

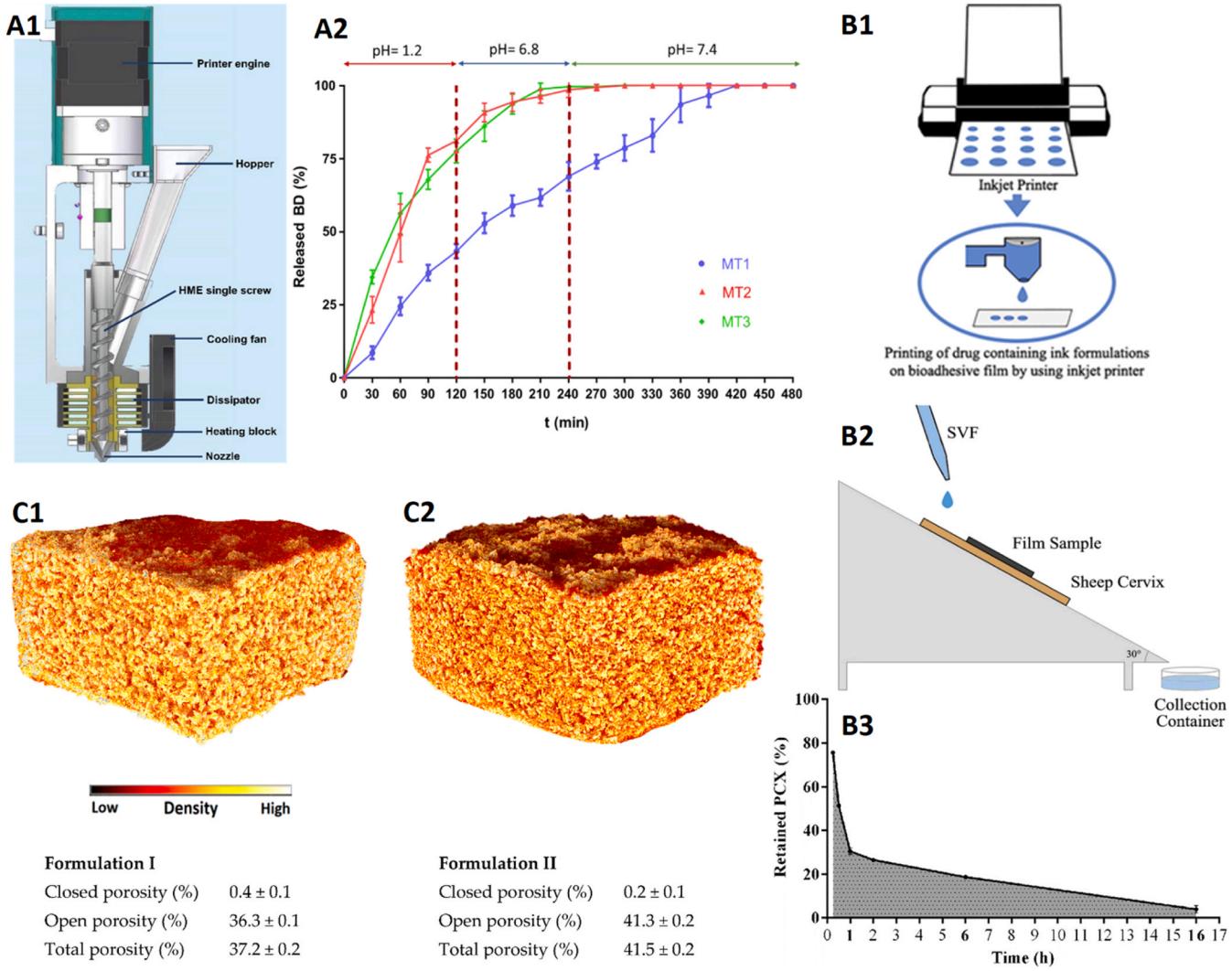

Fig. 4. (A1) Schematic draw of a direct powder extrusion (DPE) 3D printing head; (A2) budesonide (BD) release profiles from the DPE 3D printed min-tablets as a function of pH showing the faster release conferred by HP-β-CD in MT2 and MT3 formulations. Reproduced from Pistone et al. [64] with permission from Elsevier. (B1) Inkjet printing of paclitaxel:HP-β-CD inclusion complexes dispersed in water:propylene glycol 40:60 v/v mixture and printed onto HPC films; (B2) ex vivo test using simulated cervix environment to test paclitaxel release; and (B3) percentage of drug remaining in the film during the ex vivo test. Adapted from Varan et al. [66] with permission from Elsevier. (C1, C2) X-ray micro-CT images of porous ondasetron:β-CD inclusion complex (22% w/w) printlets prepared using selective laser sintering (SLS) 3D printing and different contents in excipients (Kollidon VA-64 and mannitol). Reproduced from Allahham et al. [69] (Creative Commons Attribution (CC BY) license).

absorbance of the laser light facilitating the sintering and also allows evaluating the homogeneity of components distribution. Formulation I also contained vinylpyrrolidone-vinyl acetate copolymers (Kollidon VA-64) at 25% w/w, which is in the rubbery state during laser and facilitates the particles binding, and the disintegrant mannitol at 50% w/w. In formulation II these components were added at 15% w/w and 60% w/w, respectively. A diode laser of 445 nm (blue laser, 2.3 W) was used for the sintering of 100 μm-thick layers. Both printed medicines exhibited a high porosity (Fig. 4 **C1,C2**), with a slightly higher percentage in open porosity in the case of formulation II. In any case, both formulations disintegrated in few seconds in contact with water and released >90% ondasetron in the first 5 min in simulated gastric fluid.

In sum, the information collected in Section 2 indicates that CDs can help solving biopharmaceutical problems related to drug solubility and instability and can expand 3D printing to lipophilic compounds that form inclusion complexes with CDs during the preparation of water-based semisolid masses or the melting of filaments or powders. However, more information is needed on the interactions of the CDs not only with the drug but also with other components, mainly polymers, before and during the 3D printing, in order to predict the effects that CDs may have on the mechanical properties of the inks and the final products, which in turn may determine drug release rate.

3. CDs as structural agents

The success of 3D printing depends largely on the mechanical properties of the starting materials and the printed products. For example, extrusion 3D printing relies on a fine balance of shear-dependent viscoelastic properties to enable easy, continuous material flow during printing and rapid filament hardening to achieve high design fidelity. Vat photopolymerization (VPP) requires materials that can respond quickly to light irradiation by transforming a solution into a solid-like material in a few seconds. CDs offer a number of advantages as structural components as they can form reversible supramolecular assemblies with a variety of components (form oils to polymers; see Fig. 1**B and C**), which exhibit high consistency at rest and disentangle under the application of high-shear conditions. Furthermore, CDs can increase the apparent solubility of initiators accelerating photocross-linking

reactions or participate in the reaction themselves by serving as building blocks.

3.1. CDs as stabilizers of emulsion-based inks for extrusion 3D printing

As explained in previous sections, extrusion 3D printing, also known as direct-ink-writing, demands inks that have high storage modulus at rest, rapidly decrease the viscosity to flow under mild shear stress, and rapidly recover the viscosity for shape fidelity. Therefore, for the success of the printing, the preparation of a homogeneous and stable system of adequate rheological properties is critical. 3D printing of emulsions has the advantage of incorporating substances of markedly different polarity by accommodating them into the hydrophilic or the hydrophobic phases. Emulsions can be endowed with the required rheological properties by increasing the proportion of internal phase (high internal phase emulsions, HIPEs) and adding gelling components to the continuous external phase. Nevertheless, the globules should also be stable during extrusion and drying avoiding leakage of the content. Thus, 3D printing of emulsions demands strong stabilization measures avoiding an increase in potentially toxic surfactants. Pickering emulsions, i.e. emulsions stabilized by solid particles instead of surfactants, are widely explored for food applications due to the greater stability and lower toxicity [70]. Indeed, 3D printing of HIPEs found a variety of applications in the food industry as animal fat substitutes, but their potential application in biomedicine (e.g., oral delivery of personalized doses) is still to be unveiled.

Due to its amphiphilic behavior, CDs are prone to accumulate in the oil-water interface, partially hosting the oil into their cavities. Accumulation is enhanced by the presence of NaCl and acidic pH, as demonstrated for HIPEs prepared with Sunflower seed oil (75% w/w)

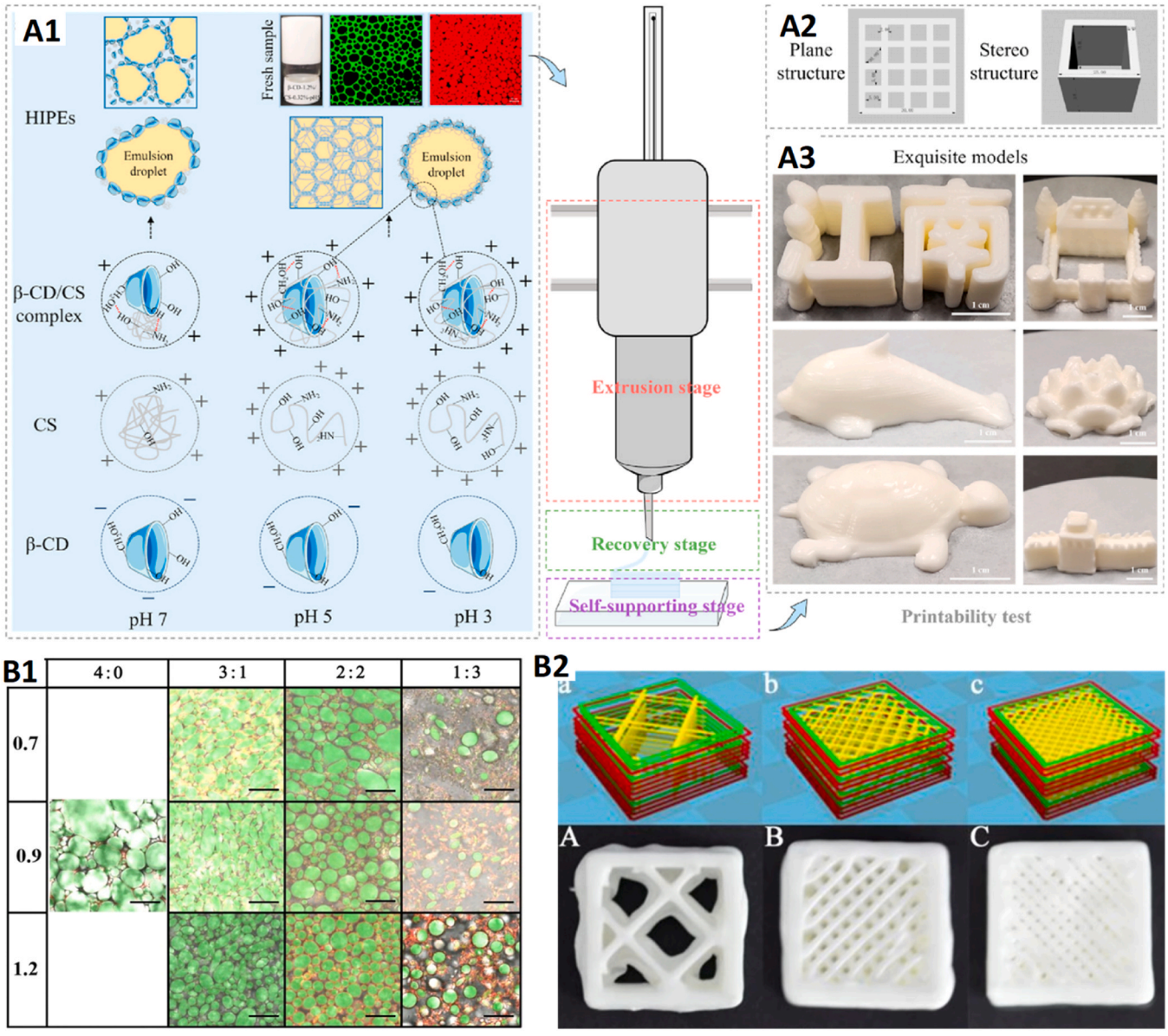

Fig. 5. (A1) High internal phase emulsion (HIPE) droplets can be stabilized using cationically charged complexes of β-CD:chitosan obtained by tuning the mass ratio of both components and the pH of the aqueous phase. (A2) The stabilized emulsions exhibited rheological properties suitable for extrusion 3D printing and (A3) objects of quite complex architecture could be obtained. Reproduced from Li et al. [73] with permission from Elsevier. (B1) Confocal laser scanning microscope images of emulsions prepared with Sunflower seed oil (65%), stabilized with β-CD:CMC complexes prepared with different mass ratios (first row) and different CMC DS (first column) and stained with Nile blue A (aqueous phase, in red) and Nile red (oily phase, in green); bar = 20 μm. (B2) 3D models (a, b, c) and the actual printed products (A, B, C). Reproduced from Guo et al. [75] with permission from Elsevier.

and β-CD solution (25% w/w) with CD concentration of 1.2%. Addition of NaCl 25 mM caused a remarkably decrease in droplet mean size from >60 μm (recorded in the absence of NaCl) to 40 μm. The highest shape fidelity of 3D printed objects (nozzle 0.8 mm; room temperature) was achieved at pH 3–4 [71]. Interestingly, 4D printed objects with a color that evolved as a function of temperature and time were prepared by adding curcumin to the oil droplets and $NaHCO_3$ to the aqueous phase. Curcumin exhibited a pH sensitive color that changed from yellow (pH 1–7) to orange (pH >7.5) as the pH increased when $NaHCO_3$ decomposed under heating at 85 ºC for 10 min. Higher temperatures or prolonged time caused the collapse of the structure.

To reinforce the globule stabilizing role, hybrid polysaccharide particles offer relevant advantages in terms of reduction of interfacial free energy and also tunability of the rheological properties [72,73]. β-CD (1.2% w/w) was mixed with chitosan at various concentration (0.08%, 0.16%, 0.24%, 0.32%, and 0.40% w/w) and pHs (from 3 to 7). Amphiphilic complexes of β-CD:chitosan that can serve as interfacial membrane were obtained at 1.2:0.32 mass ratio; the most favorable balance regarding ionic interactions was obtained at pH 5 (Fig. 5 **A1**). HIPEs prepared with sunflower seed oil (75 g) and β-CD:chitosan solution (25 g) exhibited adequate self-healing properties and were 3D printed (nozzle diameter of 0.80 mm) in a variety of elaborated shapes with high fidelity (Fig. 5 **A2-A3**) [73]. The interactions between β-CD and chitosan were shown to be reinforced, as well as the strength of the gel-like inks, by chemical modification of β-CD with anionic groups (through reaction with octenyl succinic anhydride [74].

Complexes of β-CD and carboxymethylcellulose (CMC) have also demonstrated good performance as steric and electrostatic barrier on the droplets. In water, β-CD and CMC spontaneously assembled, probably driven by hydrogen bonding, as 1 μm size aggregates with negative Zeta-potential, which was more negative as the DS of CMC increased from 0.7 to 1.2. Pickering emulsions with Sunflower seed oil phase content of 65% were readily formed using β-CD:CMC 2:2 mass ratio; as the degree of substitution (DS) of CMC increased, the droplets became more regular, smaller and denser (Fig. 5 **B1**) [75]. Differently, CMC solely (without β-CD) failed to stabilize the droplets as this polysaccharide cannot form colloidal particles by itself. Pickering emulsions prepared with the optimum β-CD:CMC 2:2 mass ratio and CMC DS 1.2 needed a bigger force to start flowing but also exhibited marked shear thinning behavior, which facilitated the subsequent 3D printing as cuboids (20×9.5 mm) with filling densities ranging from 20% to 100% (Fig. 5 **B2**). The printing was carried out at 25 ºC through 0.80 mm nozzle and the obtained objects showed good shape fidelity. Similarly, mixtures of β-CD and citrus pectins 2:2 mass ratio have recently demonstrated to form negatively charged aggregates (1–2 μm size) that efficiently stabilized HIPE droplets and communicated the adequate rheological properties for extrusion 3D printing [76].

Pickering emulsions stabilized with cellulose nanocrystals have recently been endowed with self-supportive properties using poly (pseudo)rotaxanes of poly(ethylene glycol), PEG, and α-CDs, by forming a supramolecular gel in the oil-water interface [77]. The 3D printability of these systems has not been explored for drug delivery yet. Poly (pseudo)rotaxanes and other CD-based supramolecular gels are further developed in next section.

3.2. Poly(pseudo)rotaxanes and zipper-like assemblies

CDs can be threaded by a variety of polymers having repeating units small enough to accommodate inside the CD cavity, forming poly (pseudo)rotaxane (Fig. 1**Ca**). Typically, poly(ethylene glycol), PEG, easily forms poly(pseudo)rotaxanes with α-CDs, while poly(propylene oxide), PPO, and polyalkyl chains with a larger cross-sectional area fit into β-CDs [78,79]. Two chains of PEG can accommodate into a γ-CD. Thus, depending on the size of the polymer and the CD, poly(pseudo) rotaxanes exhibiting different properties can be obtained, as extensively reviewed elsewhere [37]. Relevantly for 3D printing, threading of α-CDs through hydrophilic polymers or blocks of multiblock copolymers causes a decrease in the hydrophilicity, which triggers a coacervation process. Threaded α-CDs arrange head-to-head and tail-to-tail along the polymer. α-CDs of adjacent poly(pseudo)rotaxanes may stack forming nanocylinders with a crystalline channel type structure, which results in strong supramolecular gels. The interactions among the poly(pseudo) rotaxanes are highly dynamic; namely, under mild stress (e.g., the pressure in the 3D printer barrel), the interactions among α-CDs are broken, the supramolecular assemblies disintegrate, the viscosity drops, and the individualized poly(pseudo)rotaxanes can easily flow. Once the stress stops, the poly(pseudo)rotaxanes re-assemble again and the supramolecular gel is recovered. The rheological properties of the poly (pseudo)rotaxane-based supramolecular gels relay mainly on the strength of the microcrystalline domains formed by the stacking of the CDs participating in the threading of guest polymers. Unfortunately, in most cases these supramolecular gels are extrudable but not self-supportive by themselves as they exhibit thixotropic properties and require time for a full reassembly [80].

Instead of using free CDs, polymers bearing CD moieties can readily interact with polymers bearing side chemical groups or small chains that fit into the CD cavities (Fig. 1 **Cc**). This association remembers a zipper-like assembly, in which the host-guest binding affinity (equilibrium constant) determines the strength and also the reversibility of the cross-linking points. The zipper-like assemblies may transform short polymers and oligomers into well-structured 3D networks, exhibiting self-healing capability [81]. The dynamic binding of the CD-containing polymer and the guest-bearing polymer also allows rapid disentanglement under shearing to easily flow through small diameter nozzles. When the stress disappears (rest conditions on the printer platform) the zipper-like assemblies are rapidly reformed, conferring shape fidelity after extrusion.

In general, CD-based dynamic cross-linking is very sensitive to a variety of stimuli that alter the conformation of the guest and thus switch the threading or the zippering on and off [82]. Secondary stabilization of the poly(pseudo)rotaxanes and the zipper-like assemblies is feasible through photo-crosslinking of reactive groups, applying UV-light post-processing techniques coupled to the 3D printer [83] or through secondary chemical cross-linking [84], as described in the next paragraphs.

3.2.1. Poly(pseudo)rotaxanes

Poly(pseudo)rotaxane formation has been used to prepare bio-inks of PEGylated chitosan, α-CDs and gelatin. The inks were stabilized by the microcrystalline assemblies of the α-CDs threaded along the PEG chains, and then reinforced by β-glycerophosphate that chemically cross-linked the gelatin (Fig. 6 **A**). The combination of poly(pseudo)rotaxanes and gelatine communicated shear-thinning properties to the inks, which could accommodate mesenchymal stem cells to be bioprinted at 15 ºC in the form of cylindrical scaffolds (10 mm diameter x 3 mm thickness; 2 mm pores). The scaffolds were then immersed in β-glycerophosphate solutions of different concentrations (0.3–1.3 M) for 10 min and then washed with culture medium; increasing the concentration of β-glycerophosphate, the strength of the printed hydrogels increased too but the pore size decreased. These changes determined the differentiation of stem cells to neural cells in the less cross-linked scaffolds and to adipocytes in the more cross-linked ones [85].

Poly(pseudo)rotaxanes can also be obtained by threading of α-CDs on PEO-PPO-PEO block copolymers. Adding a large proportion of α-CDs (10–20% w/w) to PEO-PPO-PEO (5% w/w) micelles, 3D supramolecular structures of micelles assembled in the core through the PPO blocks and cross-linked in the shell by poly(pseudo)rotaxanes can be formed [86]. The obtained supramolecular gels are highly viscoelastic, but the self-healing properties are not sufficient for a fast recovery upon shear stress. To overcome this problem, PEO-PPO-PEO can be methacrylated at both ends. Thus, after extrusion 3D printing, UV-light induced secondary cross-links (Fig. 6 **B**). The contribution of poly(pseudo)rotaxane crystalline domains to the mechanical properties of the scaffolds was

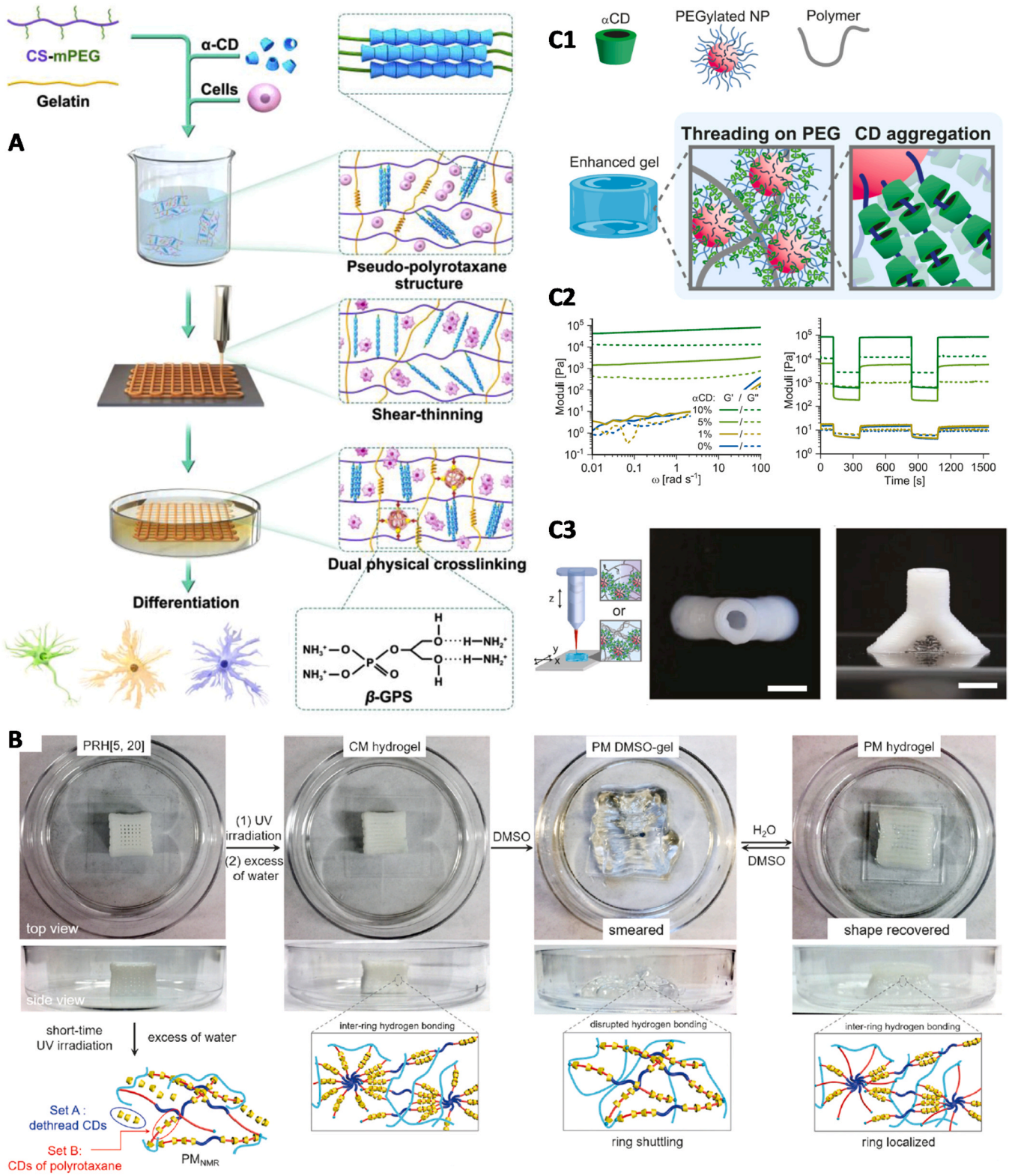

Fig. 6. (A) Preparation of a bio-ink of PEGylated chitosan, α-CDs, gelatin and mesenchymal stem cells in which poly(pseudo)rotaxane formation confers extrudability and self-supportive properties during 3D printing; the scaffolds were immersed in β-glycerophosphate solutions (β-GPS) of different concentrations (0.3–1.3 M) to reinforce the mechanical properties, which in turn determined the differentiation of the cells to different lineages. Reproduced from Hu et al. [85] with permission from Elsevier. (B) 3D printed wood-pile lattice cubes (top and side views) fabricated using poly(pseudo)rotaxanes of α-CDs (20% w/w) and methacrylated PEO-PPO-PEO micelles (5% w/w) designed as PRH [5,20] as freshly prepared, after photopolymerization (CM), immersion in DMSO, and washing in water. Reproduced from Lin et al. [87] with permission from John Wiley and Sons. (C1) Supramolecular polymer-nanoparticle (PNP) hydrogels reinforced by threading of α-CDs on the PEGylated nanoparticles and subsequent poly(pseudo)rotaxane formation; (C2) the addition of α-CDs at 5% or 10% w/w increased the values of both moduli and endowed the hydrogels with excellent recovery after stress. (C3) The inks showed excellent shape-fidelity after extrusion 3D printing of a miniaturized trachea (32 layers). Adapted from Bovone et al. [89] (Creative Commons CC-BY-NC license).

evidenced by immersion in dimethylsulfoxide (DMSO). In DMSO, the crystalline domains broke and the scaffold smeared and swelled. Re-immersion in water allowed for the re-formation of the crystalline domains and the recovery of the initial shape [87].

Supramolecular structures have also been used as templates to generate 3D printed solely CD networks. Poly(pseudo)rotaxane-based inks were prepared with bis-triethoxysilane-based telechelic PEG (PEG-2Si(OEt)) (6% w/v) and α-CDs (27% w/v). After extrusion 3D printing, the siloxane groups underwent polycondensation in a NH_3 atmosphere, and then the α-CDs threaded on the same PEG axle (preferentially) or on two different PEG axles (least likely) were chemically cross-linked using 2,4-toluene diisocyanate. Finally, the PEG chains were removed, and an urethane-crosslinked network of α-CD nanotubes was obtained. These 3D printed structures were shown useful as traps for selective recognition of molecules that are larger than CD cavities or that require several CDs to form inclusion complexes [46].

α-CDs have been shown useful for the supramolecular reinforcement of polymer-nanoparticle (PNP) hydrogels. Nanoparticles decorated with adequate polymer chains protruding to the aqueous phase (e.g., PEGylated nanoparticles) may form well-structured hydrogels when mixed with polymers (e.g., HPMC) able to interact with those side chains [88] [89]. A miniaturized trachea was 3D printed with an ink of α-CDs (7.5% w/w), PEG-b-PLA nanoparticles (5% w/w) and collagen (0.4% w/w, instead of HPMC) (Fig. 6 **C3**). Using methacrylated hyaluronic acid (1% w/w) instead of collagen, the 3D printed objects could be reinforced by photo-induced cross-linking.

3.2.2. *Zipper-like assemblies*

Bio-inks for 3D printing have been prepared using mixtures of hyaluronic acid (HA) functionalized with either adamantane or β-CD that assembled as weak zipper-like gels [83]. Adamantane forms a stable inclusion complex with β-CD with a high binding constant of approx. 3.5×10^4 M^{-1} [90]. The 3D printing was carried out applying two different strategies (Fig. 7 **A1-A2**): (a) injection of the zipper-like gel into a preformed soft hydrogel (support hydrogel) [91], and (b) modification of HA with methacrylate groups for UV cross-linking of direct 3D printed layers of the zipper-like gel [92]. Michael-type addition can be used for further reinforcement of the 3D structure by modifying some adamantane-HA chains with thiol groups that react with available methacrylate groups in the cyclodextrin-HA chains [83]. Recently, microgels of HA modified with adamantane and β-CD have been shown suitable to encapsulate cells in the spaces between the microgels preserving cell viability against high shear conditions, which may find application in cell-based therapies [93]. Another approach to combine β-CD-adamantane interactions and UV cross-linking consisted in mixing acrylate derivatives of β-CD and adamantane (9% w/w) with

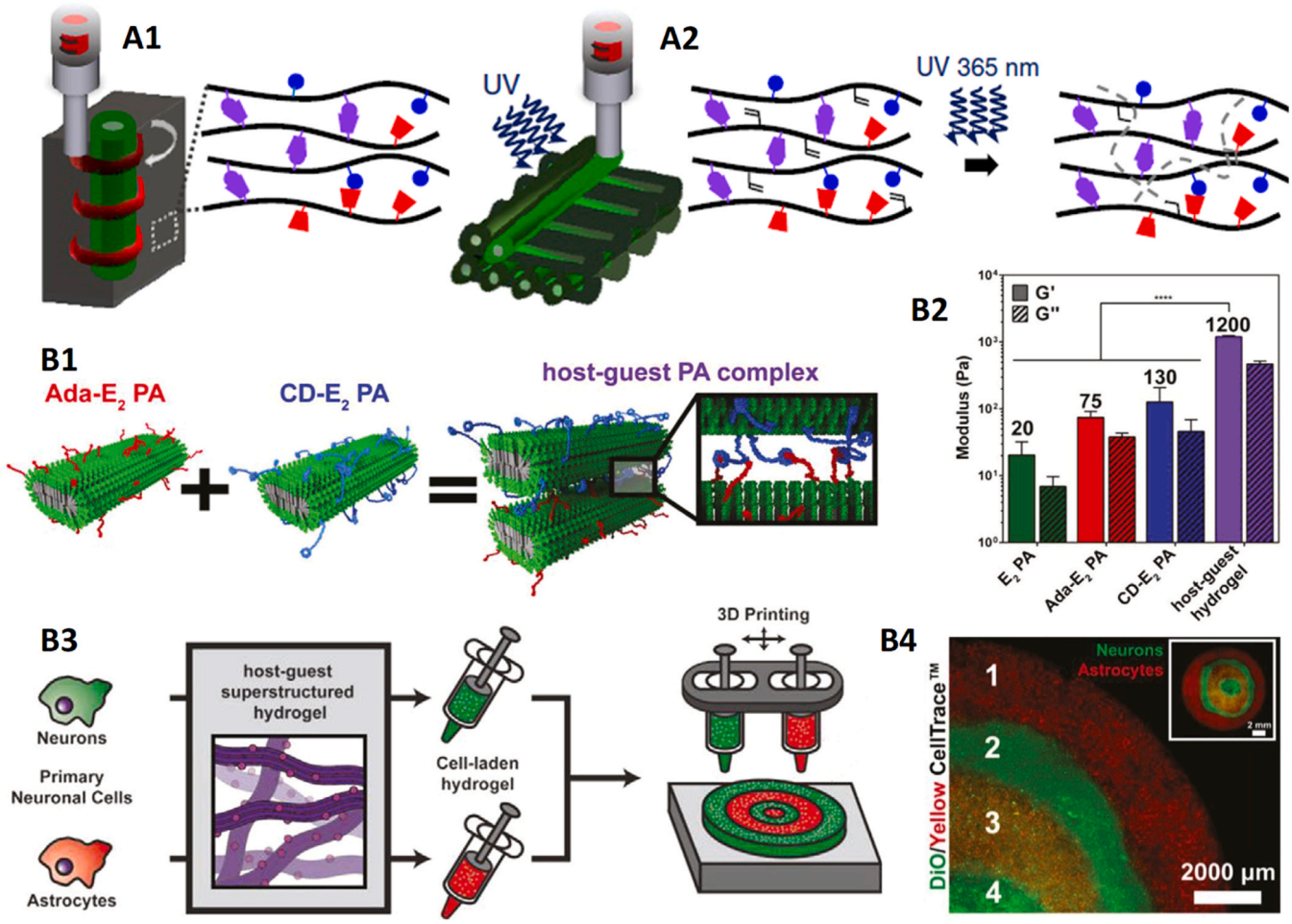

Fig. 7. Extrusion 3D printing of (A1) zipper-like assemblies of polymers bearing β-CDs and adamantane into a support hydrogel, and (A2) methacrylated polymers that form zipper-like assemblies and are extruded as layers that are stabilized by UV exposure in the presence of a photoinitiator. Adapted from Loebel et al. [83] with permission from Springer Nature. (B1) Preparation of nanofibers of peptide amphiphiles containing adamantane (Ada-E_2 PA) or β-CDs (CD-E_2 PA) that assembled when mixed; (B2) the host-guest formed hydrogels showed rheological properties that are adequate to serve as (B3) bio-inks that can include neuronal cells. (B4) Cell-laden bio-inks were printed following concentric patterns with high fidelity. Adapted from Edelbrock et al. [97] with permission (Creative Commons CC BY license).

methacryloyl gelatin (15%) and Irgacure 2959 (0.5%). 3D scaffolds were obtained by extrusion 3D printed (platform at 5 ºC) combined with photopolymerization (10 mW/cm^2) for 3 min [94]. Regulating the acrylate substitution in the β-CD and adamantane allows obtaining dually host-guest and chemically cross-linked hydrogels even in the absence of a third monomer [95]. Relevantly, if the hydrogel structure is damaged under stress or by cutting and the host-guest inclusion complexes are broken, they can be easily reorganized when the stress ceases and the hydrogel structure can rapidly heal. Similarly, alginate modified with adamantane or β-CD formed extrudable gels that were mechanically reinforced through ionic cross-linking using Ca^{2+} ions [96].

Host-guest interactions between β-CD and adamantane have also shown to reinforce the self-assembly of peptide amphiphiles (PA) providing mechanically robust hydrogels adequate for 3D printing [97] [97].

3.3. Acrylic derivatives

Light-induced polymerization offers a wide range of possibilities for the 3D printing of medicines and medical devices with very versatile and precise internal and external architectures [98,99]. This technique is known as vat photopolymerization (VPP) and includes stereolithography (SLA), digital light processing (DLP), continuous liquid production interface (CLIP), computed axial lithography (CAL) and two-photon polymerization (2PP), as reviewed elsewhere [100]. Vat polymerization 3D printing requires monomers that undergo radical polymerization in the presence of an adequate photoinitiator. The object can be made with a continuous composition using the same ink for all light-exposed layers or with a different composition in each layer by manually or automatically switching the vat. Gradient composition could also be produced by using multi-material syringe pumps or through microfluidic resin dispensing systems [98]. The environmental impact of vat polymerization, which can proceed in water environment or absence of solvents and does not require heating, may notably benefit from further development of bio-sourced monomers and cationic photopolymerization [101].

CDs have been pointed out as a tool to obtain greener polymers because of their capability to form inclusion complexes with hydrophobic monomers and thus enabling the polymerization reactions to occur in aqueous medium [102]. CDs used as monomer solubilizer are not usually included in the synthesized polymer, as they are removed from the growing chains and thus can be reused for subsequent polymerizations. Similarly, CDs may solubilize poorly water soluble photoinitiators, which are usually more efficient than the hydrophilic counterparts and allow for faster processing [103]. As an example, HP-β-CD forms inclusion complexes with 2,7-bis(2-(4-pentaneoxyphenyl)-vinyl)anthraquinone initiator, which in aqueous medium showed a two-photon absorption at 780 nm. The inclusion complex can be stored as a freeze-dried powder that easily disperses in water-based inks for fast 3D printing [104].

In addition to this role as mediator of polymerization, CDs can serve as the building blocks of the polymers and also act as cross-linkers. Functionalization of the hydroxyl groups of CDs with vinyl or (meth) acrylate moieties transforms CDs into reactive monomers for photocurable inks. Each glucopyranose unit of CD bears -OH in positions 2, 3 and 6, and thus α-CD, β-CD and γ-CD offer 18, 21 and 24 available hydroxyl positions for substitution. Preparation of monosubstituted CDs is difficult due to the similar reactivity of the -OH groups placed in the same position of the glucopyranose ring. Namely, β-CD can be readily prepared with 7, 14 or 21 reactive double bonds under the right synthesis conditions. In general, -OH in C6 of the primary face is the most nucleophilic, most basic and reactive; differently, -OH in C3 is the most inaccessible and less reactive [105].

Multiacrylated γ-CD was obtained via reaction with acryloyl chloride. This monomer (at 10%, 20% and 30% w/w) was either used as the solely component of the ink dissolved in propylene carbonate (PPC) or as a comonomer with methacrylated polyethylene glycol (PEGMEM) which also served as solvent (Fig. 8 **A**) [40]. Using phenylbis(2,4,6-trimethylbenzoyl)phosphine oxide (BAPO-Ph; 0.5% w/w) as initiator and methyl-red (0.05% w/w) as a dye to regulate light diffusion, the photopolymerization was shown to occur in few second due to an autoacceleration phenomenon triggered by the close proximity of the reactive double bonds. Indeed, multiacrylated γ-CD solely networks were excessively cross-linked and produced too rigid and brittle object. Thus, an adequate printing required the dilution effect of linear PEGMEM. More "green" inks were obtained by replacing PEGMEM with methacrylated starch obtained from maize starch [106]. The obtained networks were found suitable for removing aquatic pollutants, such as methylene blue. Suitability for 3D printing was demonstrated by the high-fidelity reproduction of the CAD models when each layer was irradiated for just 2.5–3.0 seconds.

In the field of regenerative medicine, acrylamide-β-cyclodextrin (β-CD-AAm) microgels have been tested as an alternative to the complex operations that conventional preparation of cell spheroids involves [107]. The microgels were prepared by inverse emulsion polymerization and assembled as a porous hydrogel in the presence of poly (N-isopropylacrylamide) (PNIPAm) (Fig. 8 **B1-B2**). Host-guest interactions occurred between the β-CD cavities and the isopropyl groups of PNIPAm conferring self-healing properties to the hydrogel. Adipose derived stem cell (ASC) readily grew on the hydrogel walls and aggregate forming the spheroids in the hydrogel pores. The hydrogel was swollen at room temperature, loaded with chondrocytes, and 3D printed trough extrusion to form small tubes. In culture medium at 37 ºC the 3D printed tubes shrank and favored the development of cartilage-like tissue, which was shown suitable to be implanted in vivo.

In sum, the information collected in Section 3 indicates that CDs can help address a variety of physicochemical and mechanical demands during 3D printing, such as HIPE stabilization, shear-responsive viscoelastic properties of masses for extrusion 3D printing, and improved photocross-linking reactions in aqueous-based environments. However, there is still a lack of information on the stability of the CD-stabilized 3D printed products (shelf life) and how environmental variables such as temperature, humidity, oxygen or light can alter the properties of the materials before and after printing. Also, in the case of VPP, a better understanding of the how the formation of inclusion complexes modifies the reactivity rate could allow a rational selection of the components (initiators, co-monomers).

4. CDs as responsive components for 4D printing and wearable sensors

As mentioned in the Introduction, 3D printed objects can benefit from the evolution of their properties as a function of time. Thus, unlike conventional 3D printing of objects that must not vary their morphological characteristics, 4D printing seeks to exploit the sensitivity to surrounding environmental variables to prepare objects that better develop a certain function or that serve as sensors. Typical examples refer to implantable devices that are inserted into the body using minimal surgical interventions and that expand and adopt the right morphology after implantation [108,109]. Most 4D printed objects rely in shape memory polymers and shape morphing hydrogels [110]. In the food industry, CD-based capsules loaded with essences and pigments are printed as 3D objects that break under heating in a microwave changing the color or smell. This 4D printing is being explored as a way of making the food tastier [111], but the role of CDs on the responsiveness to the heating is unclear. Similarly, color changes in 3D printed food as a function of pH driven by the presence of a color indicator (e.g. curcumin) have been reported [112]. Examples of how CDs can play the leading role in 4D behavior are discussed in the following paragraphs.

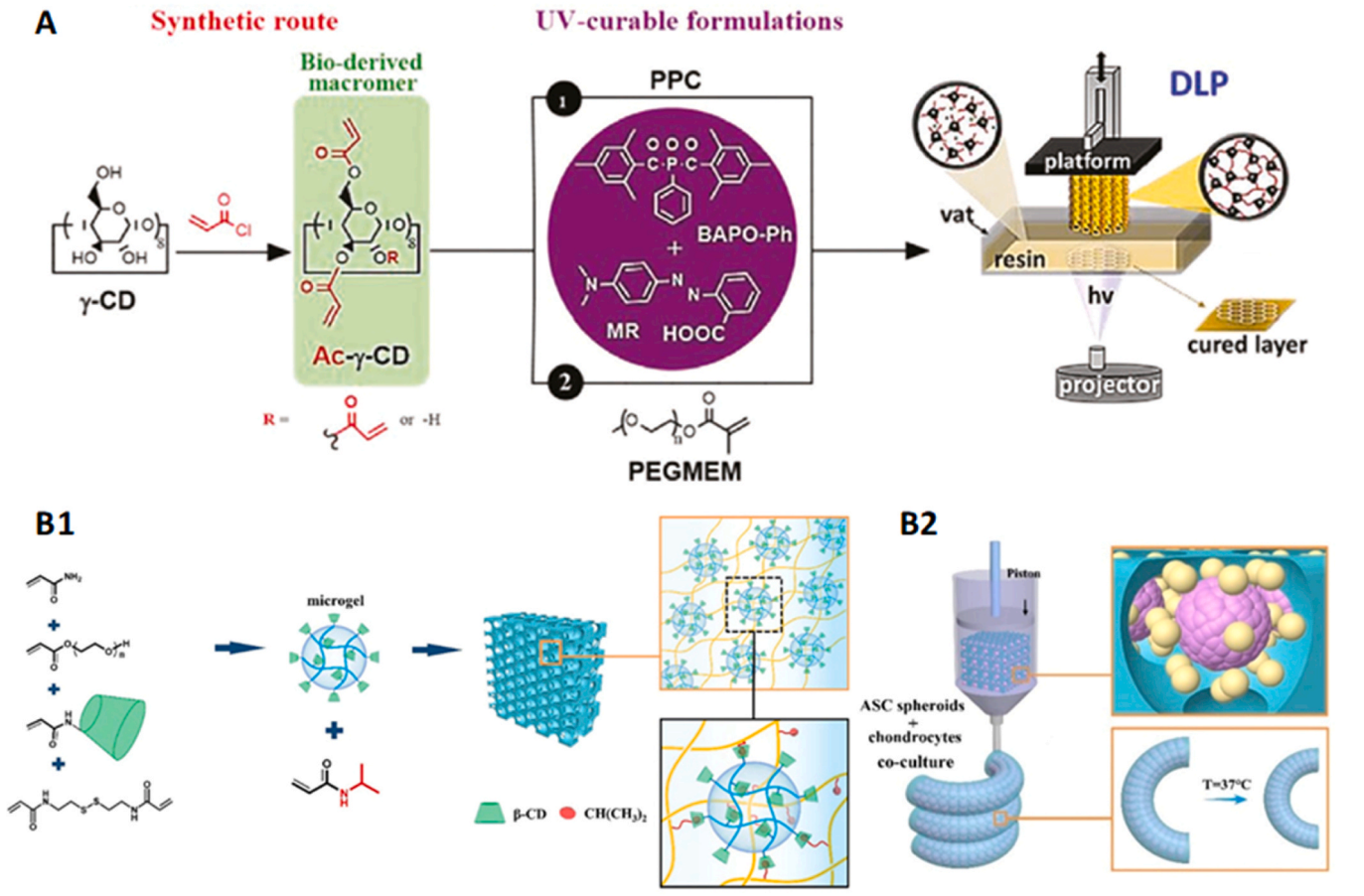

Fig. 8. (A) Multiacrylated γ-CD was used as main component of inks for digital light processing (DLP) 3D printing either (1) dissolved in propylene carbonate (PPC) or (2) as a comonomer with methacrylated polyethylene glycol (PEGMEM). Phenylbis(2,4,6-trimethylbenzoyl)phosphine oxide (BAPO-Ph; 0.5% w/w) was used as initiator and methyl-red (0.05% w/w) as a dye to regulate light diffusion. Reproduced from Cosola et al. [40] with permission from John Wiley and Sons. (B1) Acrylamide-β-cyclodextrin was mixed with acrylic monomers and cross-linker to form microgels that can interact with the isopropyl groups of poly (N-isopropylacrylamide) and form a porous hydrogel. (B2) This hydrogel served as scaffold for the growth of adipose derived stem cell (ASC) spheroids (in pink) and also hosted chondrocytes (in yellow), and it was then 3D printed trough extrusion at room temperature to form small tubes. The printed scaffold showed temperature-responsiveness due to poly(N-isopropylacrylamide) and favored the development of cartilage-like tissue when cultured at 37ºC. Reproduced from Zhang et al. [107] with permission from IOP Science.

4.1. Moisture sensitiveness

The number of CDs and the rate at which they thread along a polymer significantly determine the properties of the final supramolecular network. The higher the density of crystalline cross-linking points, the lower the swelling of the 3D printed object. Combination in the same object of regions printed with inks differing in the poly(pseudo)rotaxane density causes a non-homogeneous (anisotropic) swelling of the object, which may distort its shape and size [113].

Regulation of the kinetics of poly(pseudo)rotaxane formation appears as a versatile tool to confer the desired properties to a 3D printed object. It has been shown that bulky groups placed at the ends of the polymer to be threaded may notably delay the poly(pseudo)rotaxane formation acting as "speed bumps" [114]. Also, placing bulky blocks in between threadable blocks allows regulation of the supramolecular gel properties [115]. Meta-stable materials based on poly(pseudo)rotaxanes have the advantage of remaining in the desired conformation for longer time, compare to other meta-stable materials, making the achievement of a wide range of complex functionalities possible. The conventional threading of PEGs by α-CDs occurs very rapidly (less than 15 min at 20 ºC) as the energy barrier is low, while packaging of the poly(pseudo) rotaxanes and crystallization is a much slower process (rate-determining step) (Fig. 9 **A1**). PEG chains grafted with "speed bumps" show very slow threading (>100 min for PEG-adamantyl ester or PEG-norbonylester) as the energy barrier raises; the α-CDs can only be threaded from one PEG end or very slowly from both ends, which enables a precise kinetic control of the number of α-CDs that form each poly(pseudo)rotaxane (Fig. 9 **A2-A3**). The unidirectional movement of α-CDs along PEG is slow and also the translocation because the coiled conformation of PEG axle causes an additional energy barrier. In comparison, the crystallization of α-CDs of adjacent poly(pseudo)rotaxanes occurs faster, which allows trapping the meta-stable conformation of the kinetically controlled poly (pseudo)rotaxanes. Interestingly, the crystallization of the smaller and more segmented α-CD domains produced much stronger hydrogels than the homogeneous poly(pseudo)rotaxanes, which favored 3D printing. The kinetic controlled poly(pseudo)rotaxanes can be made permanent after printing by means of a tetrathiol cross-linker and a photo-initiator [113].

The temperature has also shown to determine the threading of α-CDs along PEG-norbonylester as an increase in temperature causes the de-threading of some CDs. Thus, inks printed at 60 ºC (designed as PNH-3) have lower PEG:α-CD molar ratio (1:3) and smaller Youngś moduli (14 kPa) compared to those printed at 20 ºC (designed as PNH-8) that had PEG:α-CD 1:8 molar ratio and Youngś moduli of 180 kPa (Fig. 9 **A4**). As a consequence of the looser structure, PNH-3 swelled 270% when stored at relative humidity (RH) of 58%, while swelling of the PNH-8 was significantly lower. This different response to humidity allowed the preparation of 3D objects that exhibited different folding capabilities

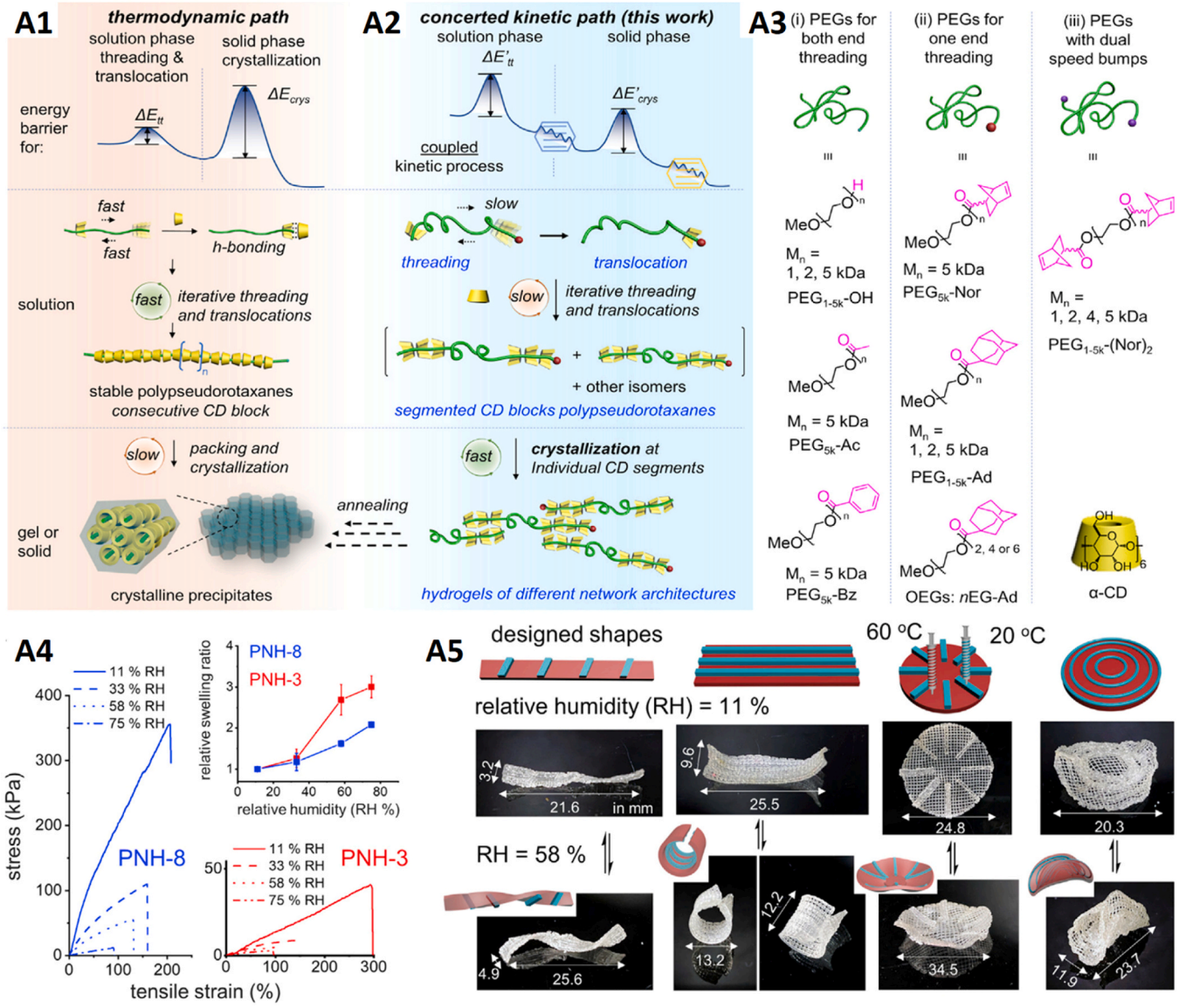

Fig. 9. A comparison between (A1) conventional, thermodynamic-controlled poly(pseudo)rotaxane formation (fast) and supramolecular assembly (slow) and (A2) kinetic-controlled formation of meta-stable poly(pseudo)rotaxane via slow threading and translocation of α-CDs on the PEG axle and subsequent stabilization of the network through the crystalline assemblies. (A3) PEGs and oligoethylene glycols (nEG-Ad) with bulky ends (e.g. adamantly ester and norbonylester) that act as speed bumps. (A4) Tensile stress measurements of PNH-3 and PNH-8 hydrogels and their swelling ratio recorded after being exposed to environments of different relative humidity (RH). (A5) Designed models and printed objects that combined PNH-8 (printed at 20°C; green) and PNH-3 (printed at 60 °C; red) and their changes in morphology in environments of RH 11% and 58%. Reproduced from Lin et al. [113] with permission from Elsevier.

according to a predesigned pattern. The objects were constructed using the same ink but in some regions the ink was printed at 20 °C and in other regions at 60 °C (Fig. 9 **A5**). After printing, each poly(pseudo) rotaxane conformation was made permanent by means of UV-photopolymerization [113].

Poly(pseudo)rotaxanes have also been explored to endow 3D printed objects with modifiable mechanical properties, mimicking the capability of certain animals such as the sea cucumber to reversibly change the stiffness of their skin to regulate water content and to protect against predators [116]. To do that, polymers were designed with PEG side chains to form poly(pseudo)rotaxanes with α-CDs only at the side chains. The mechanical properties of the inks were regulated by tuning the length and density of the PEG side chains and α-CDs concentration [117]. After 3D printing, the structure was reinforced through photo-crosslinking of the backbone polymer. Since the poly(pseudo) rotaxanes were not covalently cross-linked, the mechanical properties of the 3D printed objects were very sensitive to de-threading and re-threading of α-CDs by simple dilution in water or re-immersion in α-CDs solutions, respectively. Combining different poly(pseudo)rotaxane inks in the 3D printed object spatiotemporal changes in the mechanical properties could be achieved. Biomedical applications of such a performance are still to be explored.

4.2. Body temperature

Small-diameter vascular stents (<6 mm) are increasingly needed to improve vascular lower limb blood supply. Stents made of shape memory polymers could allow for smaller incisions and lesser risk of thrombosis and embolism [118]. To be suitable for implantation, the shape memory polymers should undergo the transition at body temperature. PCL with a start configuration was synthesized using β-CD as a core and bearing 21 arms of PCL with acrylate end groups. This

β-CD-g-PCL was used as the ink for simultaneous 3D printing and UV-curing at 365 nm. After the printing, two minutes more of UV light irradiation were applied to complete the photopolymerization. Scaffolds of 5 mm diameter and 10–40 mm length were obtained in few minutes. The scaffolds were able to expand and deform at 40 ºC while still showing adequate mechanical resistance. β-CD favored the wettability (contact angle of 70º compared to 129º for pure PCL) and biocompatibility of the stent with human umbilical vein endothelial cells (HUVECs) while endowed it with the capability to host paclitaxel. The scaffold showed a burst release in the first 3 days and then sustained the release for one month [119].

In a subsequent report, β-CD-g-PCL was cross-linked with poly-thiols by means of thiol-acrylate click reactions to obtain deployable 4D printed stents. In this case, in addition to serve as the main core of the polymer, β-CD was responsible for the hosting and sustained release of everolimus, which in turn attenuated the inflammatory response after implantation [120]. These scaffolds were stretched to the desired size for implantation by applying a certain pressure followed by cooling down. When the scaffolds were heated again at a temperature above body temperature, the initial length was recovered.

Temperature-responsive 3D printed hydrogels have also been prepared by exploiting the temperature-dependent solubility of methyl-α-CD. At low temperature, methyl-α-CD has higher solubility in water than α-CD because the methyl groups disrupt the hydrogen bonding among the CDs and increase the hydration number from 35 for α-CD to 90 for methyl-α-CD at 25 ºC [121]. Thus, when PEG chains are threaded by methyl-α-CD the overall hydration of the obtained poly(pseudo) rotaxanes is similar to the free PEG hydration, although the hydration of threaded PEG chains themselves is lower. An increase in temperature causes a fast dehydration of methyl-α-CD, which in turn makes the poly (pseudo)rotaxanes to aggregate forming supramolecular gels. In comparison with temperature-responsive polymers that undergo coil-to-globule transitions, the response to changes in temperature of poly(pseudo)rotaxanes of methyl-α-CD is faster since the dehydratation and movements of methyl-α-CDs along the polymer axle have lower kinetic energy barrier [122]. The main limitation of this approach is that methyl-α-CD is less prone to form poly(pseudo)rotaxanes than α-CDs. This issue was overcome by using PEG/α-CDs polyrotaxanes as ink for extrusion 3D printing followed by methylation of the threaded α-CDs post-printing (Fig. 10 **A1**). After methylation, α-CDs can freely move along the PEG axle. As the temperature increases the methylated α-CDs dehydrate and interact each other along the axle; a further increase in temperature causes the crystalline aggregation of methylated α-CDs among adjacent threaded chains. This two-step changes in aggregation can be seen as a change in the 3D printed hydrogel from transparent to opaque first and from swollen to shrunk as the temperature continues increasing (Fig. 10 **A2**) [123].

4.3. pH

Polyrotaxanes sensitive to pH and ionic strength have been prepared by combining dimethacrylamide-PEG (3.5% w/w) and α-CD (20% w/w) [124]. The pH-responsiveness of the 3D printed objects, after direct-writing, UV-cross-linking and washing, relied on changes in the protonation of the stacked CDs, which in turn reversibly altered the micro-crystalline aggregation. Since the pKa of CDs has been reported to be 12.3 for primary -OH and 13.5 for secondary -OH [125], the 3D printed networks must be chemically stable even at higher pH values. In parallel, the acrylamide groups conferred responsiveness to ionic strength. Both pH and ionic strength variables caused changes in the ring-shuttling motions along the polyrotaxanes and in the swelling of the acrylamide chains, triggering multi-stage anisotropic shape changes. The 3D printed hydrogels retained the shape after printing with high fidelity in pH <9 medium (Fig. 10 **B1**). An increase in pH beyond 12.5 made the -OH groups of α-CD to be negatively charged and thus repulsions among the α-CDs occurred, which broke the micro-crystalline aggregates and favored the random movement of the α-CDs along the PEG axle. As a consequence, the 3D printed hydrogel became softer and

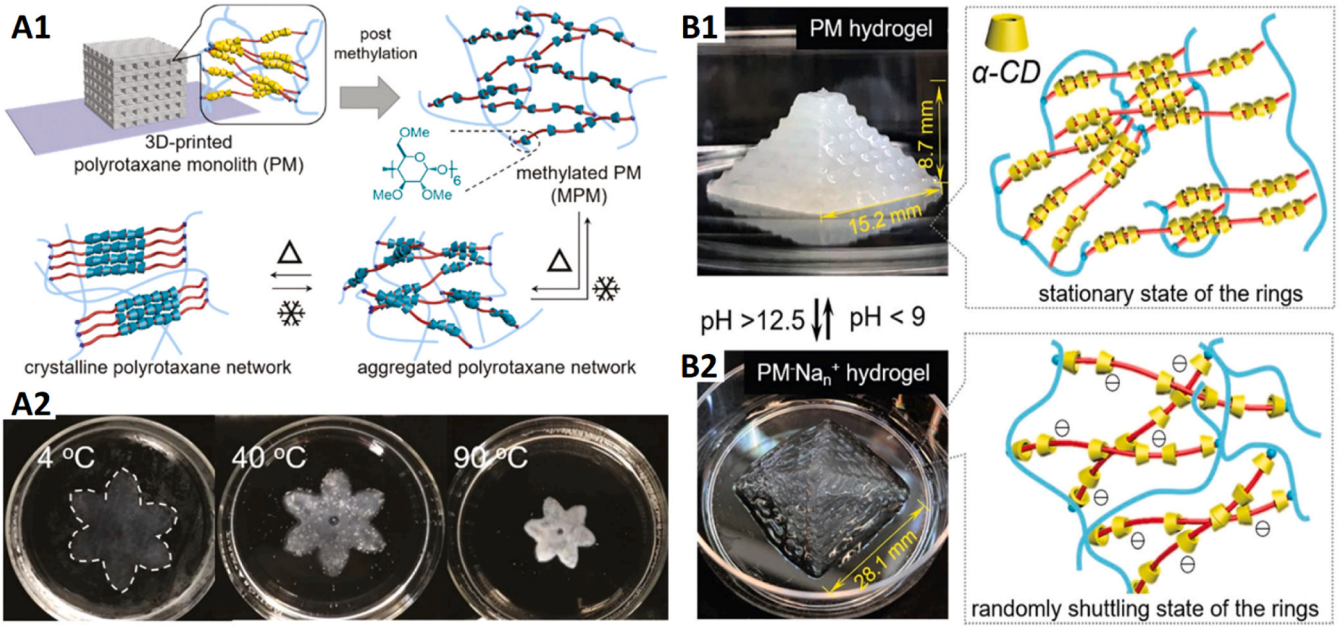

Fig. 10. (A1) 3D printed PEG/α-CD polyrotaxane-based hydrogel was subjected to methylation of the α-CDs units to confer fast temperature-responsiveness. Methylated α-CDs are more hydrophilic and move along the PEG axle. As the temperature increases and the system dehydrates, the methylated α-CDs first arrange along the axle and then participate in the crystalline aggregation of the polyrotaxane chains. (A2) This temperature-induced changes in aggregation are macroscopically transmitted as a change from transparent to opaque at 40ºC and the shrinking of the 3D printed hydrogel at 90ºC. Reproduced from Lin et al. [123] with permission from the Royal Society of Chemistry. (B1) 3D-printed pyramid obtained with a dimethacrylamide-PEG (3.5% w/w) and α-CD (20% w/w) ink, which exhibited self-supportive properties after UV cross-linking. At pH below 9, the crystalline arrangements of α-CDs among the polyrotaxanes conferred structural integrity. (B2) An increase in pH above 12.5 triggers the ionization of α-CDs, they repel each other, and the structure is disentangled. Reproduced from Lin et al. [124] with permission from the Royal Society of Chemistry.

deformed (Fig. 10 **B2**). The process was reversible and immersion in pH <9 medium allowed recovering the initial shape. The sensitiveness to pH and ionic strength could be reinforced by copolymerization of the dimethacrylamide-PEG/α-CD poly(pseudo)rotaxanes with sodium acrylate and thus taking benefit of the responsiveness of polyacrylic acid. 3D printed hydrogels combining regions with and without sodium acrylate showed strong anisotropic pH-dependent swelling, developing very varied changes in shape [124].

4.4. Mechanochromic responsiveness

Dynamic covalent chemistry has been investigated to cross-link poly (pseudo)rotaxanes using ketoenamine bonds. The imine linkages are reversible and may reinforce the self-healing properties of the micro-crystalline domains of the poly(pseudo)rotaxanes improving their properties for extrusion 3D printing without the need for photo-crosslinking. 1,3,5-benzenetrialdehyde (BD) and 1,3,5-triformylphloroglucinol (TP) were evaluated as cross-linkers. BD provided fully reversible links quite rapidly, while using TP and heating at 60ºC the links were semi-reversible due to imine-to-ketoenamine tautomerization. In this later case, a mixture of polyrotaxanes and polypseudorotaxanes was obtained. Grafting rhodamine B and fluorescein to the PEG axles, the TP cross-linked poly(pseudo)rotaxanes showed mechanochromic response when compressed. Under cyclic loading tests, the emission of fluorescence changed. At 0% strain, the printed hydrogel emitted at 533 and 582 nm upon irradiation ($\lambda ex = 450$ nm). Upon compression, the emission at 582 nm decreased, and the emission at 533 nm increased suggesting that the distances when the dyes increased due to the reversible disentanglement of the micro-crystalline domains [126]. These changes in fluorescence could be exploited in the future as pressure sensors.

4.5. Wearable sensors

The capability of CDs to form inclusion complexes with a variety of drugs, biomolecules, and environmental contaminants make them particularly attractive to develop a variety of electrochemical sensors when combined with conducting polymers, as reviewed elsewhere [127]. Unfortunately, examples of CD-based sensor fabrication using 3D printing are still rare.

Hydrogel-based sensors should be able to undergo repeated deformations under cyclic stress without breaking. It has been shown that polyrotaxanes in which the threading CDs are covalently linked as pairs, i.e., one CD of a polyrotaxane chain with one CD of other polyrotaxane chain, can enhance the capability of the hydrogels to support large stress without breaking as the sliding rings can move and dissipate the energy (Fig. 11 **A1**). Conductive rotaxane hydrogels have recently been developed by combining acrylated β-CD with bile acid derivatives bearing polymerizable groups at both ends (Fig. 11 **A2**) [128]. The host-guest assemblies were transformed into polyrotaxanes gels via DLP 3D printing in the presence of acrylamide and conductive choline chloride (ChCl) (Fig. 11 **A3**). The host-guest assemblies provided mobile cross-linking points, which endowed the printed hydrogels with an enormous capability to be reversibly stretched (>400% strain). The stretching of the hydrogels caused an increase in the resistance, which showed a linear dependence with the strain. This finding together with an excellent electrical stability allowed detecting from tiny to large stretch signals. The polyrotaxanes exhibited bioadhesion to human skin and were highly sensitive to physiological movements. 3D printed sensors prepared with these polyrotaxanes were shown able to detect real-time human electrocardiogram signals [129].

Polyrotaxanes of polyaniline and β-CD have been found useful to prepare resistive random access memory (RRAM); i.e., a type of computer memory that works by changing the resistance across a dielectric solid-state material. The β-CD units threaded along polyaniline may serve as insulative sheaths. Compact β-CD units act as an insulated molecular wire and decrease the conductivity by 2 orders of magnitude. Polyaniline/β-CD polyrotaxanes were characterized by formation of hydrogen bonds between the aniline repeating units and the OH-6 of β-CD. These polyrotaxanes were soluble in water and offered high resistance to electric current when placed between an anode (aluminum, Al) and a cathode (ITO). However, they switched to low resistance when the voltage surpassed a certain value. The response was reversible and very fast (29 ns), and the process could be cyclically repeated. The electric current causes the protonation of polyaniline imine N. This proton doping notably enhances the conductivity of the device. The electrodes and the polyrotaxanes dielectric layer can be prepared by 3D printing to obtain flexible RRAM devices that may find application for wearable devices [129].

Only recently 3D printed stretchable conductive electrodes for wearable electronics have been prepared from inks in which zipper-like assemblies stabilized liquid metal-in-water emulsion gels [130]. The droplets containing eutectic gallium indium were stabilized using polyvinyl alcohol (PVA) chains bearing β-CD and adamantane moieties (Fig. 11 **B1**). The host-guest interactions acted as bridges among the droplets serving as dynamic cross-links and enabling extrusion 3D printing. When the 3D structure was stretched, the droplets released the liquid metal generating continuous conductive pathways (Fig. 11 **B2**). Under rest, the droplet recovered their content and performed as insulators. Repeatable cyclic changes in conductivity were obtained in a wide range of strains; the 3D printed system being very sensitive even to ultralow strains.

In sum, the information collected in Section 4 highlights the enormous potential of CDs for 4D printing. However, biomedical applications require that the stimuli-responsiveness or the evolution over time of the properties of the 3D object occurs in a range compatible with physiological or pathological values. This field is expected to evolve rapidly in the coming years.

5. Concluding remarks and perspectives

Additive manufacturing and CDs can be considered the perfect technology-material tandem. 3D printing is the appropriate technological platform to take full advantage of the ability of CDs to form inclusion complexes, creating the most suitable conditions for the formation of host-guest pairs. Advances in knowledge about the thermodynamic and kinetic control of the formation of drug/biomarker-CD inclusion complexes and of poly(pseudo)rotaxanes with peptides and polymers open up a wide range of possibilities in 3D and 4D printing.

On the other hand, the CDs transform weak inks into self-supportive and self-healing materials with the right mechanical properties for the 3D printing process. Moreover, the CDs participate in the stabilization of the manufactured objects through very varied cross-linking reactions that are easy to couple to current printers. CDs are very useful tools for very precise control of the architecture of the 3D object from the nanoscale, which provides an added value that is difficult to achieve with other materials.

The role of CDs as facilitators of the printing process, stabilizers of active substances, structural agents of the formed object, and biofunctional agents capable of specific molecular recognition and sensitiveness to stimuli can give rise to a wide variety of personalized medicines and medical devices with enhanced features. In addition, their natural origin, from a renewable source, their well-known safety profile, and their compatibility with very broad polarity solvents, including the aqueous medium, are advantageous pillars for the implementation of sustainable and environmentally friendly production processes, as demanded in the context of fourth and fifth industrial revolutions.

CDs have also been shown useful as components of gels used to fill the spaces among strands of 3D printed structures made of thermoplastic polymers and hybrid composites. In that case, the 3D printed structure acts as rigid scaffold that confers mechanical support, while the soft CD-

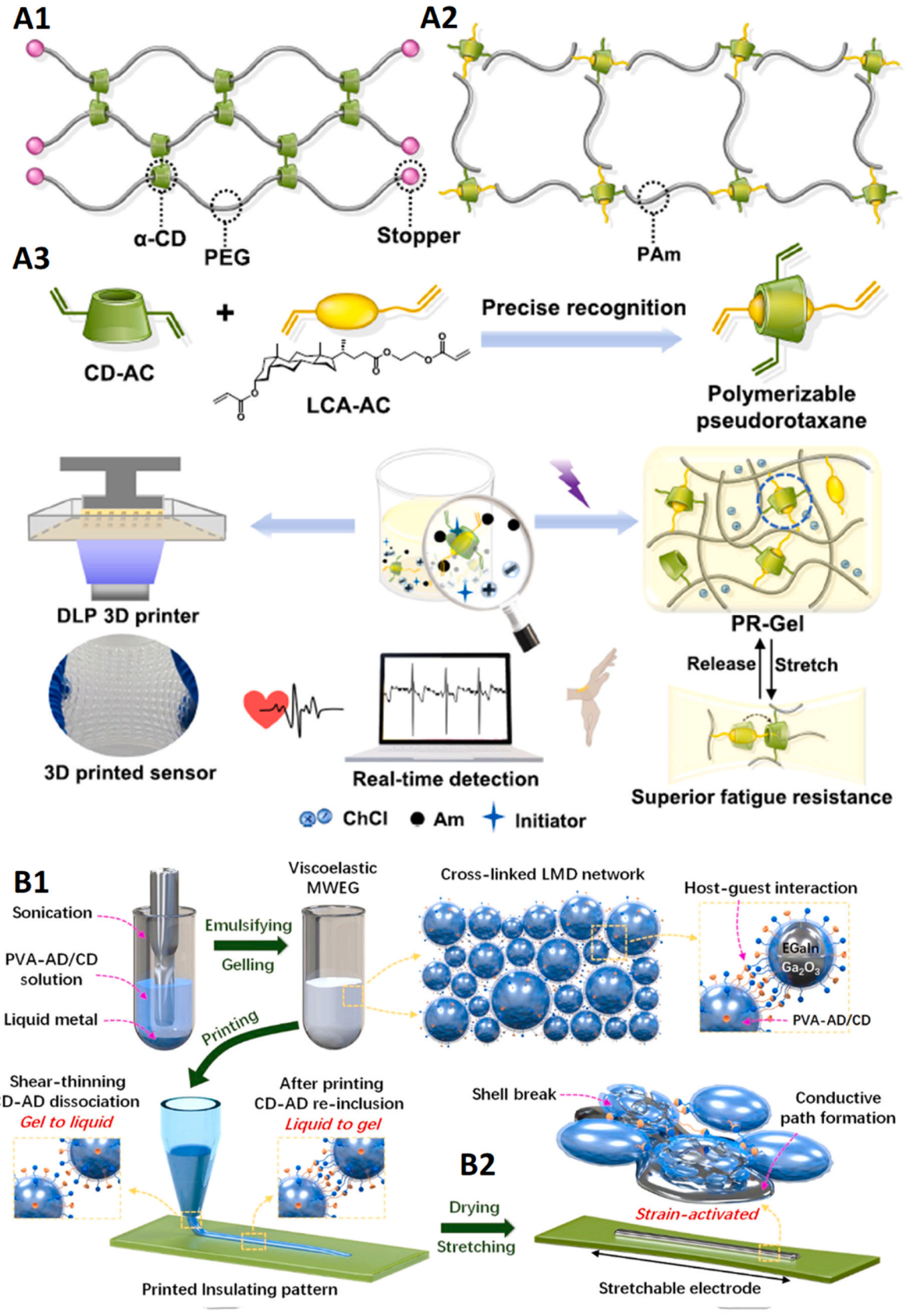

(caption on next page)

Fig. 11. (A1) Slide ring hydrogels prepared via cross-linking of CD units; (A2) slide ring hydrogels prepared via cross-linking of host-guest units. (A3) The host was acrylate β-CD (CD-AC) and the guest molecule ethyleneglycol lithocholate derived diacrylate (LCA-AC). These components were mixed with acrylamide (Am), conductive choline chloride (ChCl), an initiator (LAP), and a light absorber (tartrazine dye) for the preparation of DLP 3D printed sensors. The stretching of the hydrogels causes a rapid change in the resistance (conductivity) of the hydrogels. Reproduced from Xiong et al. [128] (Creative Commons Attribution 4.0 International License). (B1) Preparation of an emulsion of a liquid metal (eutectic gallium indium) in water using polyvinyl alcohol (PVA) chains bearing β-CD and adamantane moieties as droplets stabilizers. The CD-adamantane interactions acted as dynamic bridges among the droplets and enabled extrusion 3D printing. (B2) At rest, the liquid metal remains confined in the isolated droplets and there is no conductivity. When the printed structure is stretched, the droplets leakage the liquid metal, which creates conductive pathways. The process is reversible thanks to the rapid formation of the host (β-CD)-guest (adamantane) assemblies when the stress ceases. Reproduced from Wang et al. [130] (Creative Commons License CC-BY 4.0).

based hydrogel may provide an adequate environment for cell adhesion and proliferation while simultaneously deliver active substances that drive cell differentiation to the required lineage [131,132]. Alternatively, the very diverse techniques developed to graft CDs onto a variety of materials can be suitable for the final finishing of 3D printed objects with empty hosting cavities that may be available for a variety of host-guest interactions [133]. Moreover, the capability of CDs to form inclusion complexes with a wide range of chromophores [134] may also endow the 3D printed objects with security components to avoid counterfeit.

Overall, CDs can be considered as an emerging material in the field of 3D printing capable of contributing to the current needs for mass customization in terms of human-centricity, sustainability, and resilience. However, there is still a paucity of knowledge on the effects that the interactions of CDs with other components (oils, polymers, co-monomers) may have on the printability of the starting materials and the properties of the printed objects. The evolution over time of the printed devices and responsiveness to physio(patho)logical variables requires detailed investigation to fully exploit the biomedical applications of 4D printing. Successful preliminary results guarantee rapid evolution of the field in the coming years.

CRediT authorship contribution statement

Angel Concheiro: Writing – review & editing, Resources, Project administration, Methodology, Formal analysis, Conceptualization. **Alvaro Goyanes:** Writing – review & editing, Methodology, Formal analysis. **Carmen Alvarez-Lorenzo:** Writing – review & editing, Writing – original draft, Resources, Project administration, Formal analysis, Conceptualization.

Declaration of Competing Interest

The authors declare that they have no known competing financial interests or personal relationships that could have appeared to influence the work reported in this paper.

Data Availability

This is a review from published papers

Acknowledgements

Funding: The work was supported by MCIN/AEI/10.13039/501100011033 [PID 2020-113881RB-I00], Spain, Xunta de Galicia [ED431C 2020/17], and FEDER.

References

[1] I. Tartici, Z.M. Kilic, P. Bartolo, A systematic literature review: Industry 4.0 based monitoring and control systems in additive manufacturing, Machines 11 (2023) 712. ⟨https://doi-org.ezbusc.usc.gal/10.3390/machines11070712⟩.
[2] Breque M., De Nul L., Petridis A. Industry 5.0: Towards a sustainable, humancentric and resilient European industry. European Commision 2021. ⟨https://msu.euramet.org/current_calls/documents/EC_Industry5.0.pdf⟩.
[3] J. Leng, W. Sha, B. Wang, P. Zheng, C. Zhuang, Q. Liu, T. Wuest, D. Mourtzis, L. Wang, Industry 5.0: Prospect and retrospect, J. Manufact. Syst. 65 (2022) 279–295, https://doi.org/10.1016/j.jmsy.2022.09.017.
[4] K.P. Iyengar, E. Zaw Pe, J. Jalli, M.K. Shashidhara, V.K. Jain, A. Vaish, R. Vaishya, Industry 5.0 technology capabilities in Trauma and Orthopaedics, J. Orthop. 32 (2022) 125–132, https://doi.org/10.1016/j.jor.2022.06.001.
[5] A. Haleem, M. Javaid, Industry 5.0 and its expected applications in medical field, Curr. Med. Res. Pract. 9 (2019) 167–169, https://doi.org/10.1016/j.cmrp.2019.07.002.
[6] M. Jeyaraman, A. Nallakumarasamy, N. Jeyaraman, Industry 5.0 in Orthopaedics, JOIO 56 (2022) 1694–1702, https://doi.org/10.1007/s43465-022-00712-6.
[7] R. Godina, I. Ribeiro, F. Matos, B. T. Ferreira, H. Carvalho, P. Peças, Impact assessment of additive manufacturing on sustainable business models in Industry 4.0 context, Sustainability 12 (2020) 7066. ⟨https://doi-org.ezbusc.usc.gal/10.3390/su12177066⟩.
[8] M. Balubaid, N. Alsaadi, Achieving sustainability in manufacturing through additive manufacturing: An analysis of its enablers, Sustainability 15 (2023) 9504, https://doi.org/10.3390/su15129504.
[9] S.U. Raschke, Limb prostheses: Industry 1.0 to 4.0: Perspectives on technological advances in prosthetic care, Front. Rehabilit. Sci. 3 (2022) 854404. ⟨https://www.frontiersin.org/articles/10.3389/fresc.2022.854404/full⟩.
[10] I. Seoane-Viaño, X. Xu, J.J. Ong, A. Teyeb, S. Gaisford, A. Campos-Álvarez, A. Stulz, C. Marcuta, L. Kraschew, W. Mohr, A.W. Basit, A. Goyanes, A case study on decentralized manufacturing of 3D printed medicines, Int. J. Pharm. X 5 (2023) 100184, https://doi.org/10.1016/j.ijpx.2023.100184.
[11] L. Zema, A. Melocchi, A. Maroni, A. Gazzaniga, Three-dimensional printing of medicinal products and the challenge of personalized therapy, J. Pharm. Sci. 106 (2017) 1697–1705, https://doi.org/10.1016/j.xphs.2017.03.021.
[12] A. Awad, A. Goyanes, A.W. Basit, A.S. Zidan, C. Xu, W. Li, R.J. Narayan, R. K. Chen, A review of state-of-the-art on enabling additive manufacturing processes for precision medicine, J. Manuf. Sci. Eng. 145 (2023) 010802, https://doi.org/10.1115/1.4056199.
[13] A. Goyanes, C.M. Madla, A. Umerji, G. Duran Piñeiro, J.M. Giraldez Montero, M. J. Lamas Diaz, M. Gonzalez Barcia, F. Taherali, P. Sánchez-Pintos, M.L. Couce, S. Gaisford, A.W. Basit, Automated therapy preparation of isoleucine formulations using 3D printing for the treatment of MSUD: First single-centre, prospective, crossover study in patients, Int. J. Pharm. 567 (2019) 118497, https://doi.org/10.1016/j.ijpharm.2019.118497.
[14] L. Pugliese, S. Marconi, E. Negrello, V. Mauri, A. Peri, V. Gallo, F. Auricchio, A. Pietrabissa, The clinical use of 3D printing in surgery, Updates Surg. 70 (2018) 381–388, https://doi.org/10.1007/s13304-018-0586-5.
[15] M. Higgins, S. Leung, N. Radacsi, 3D printing surgical phantoms and their role in the visualization of medical procedures, Ann. 3D Print. Med. 6 (2022) 100057, https://doi.org/10.1016/j.stlm.2022.100057.
[16] L. Xu, H. Qin, J. Tan, Z. Cheng, X. Luo, H. Tan, W. Huang, Clinical study of 3D printed personalized prosthesis in the treatment of bone defect after pelvic tumor resection, J. Orthop. Transl. 29 (2021) 163–169, https://doi.org/10.1016/j.jot.2021.05.007.
[17] Y. Zhao, Z. Wang, J. Zhao, M. Hussain, M. Wang, Additive manufacturing in orthopedics: A Review, ACS Biomater. Sci. Eng. 8 (2022) 1367–1380, https://doi.org/10.1021/acsbiomaterials.1c01072.
[18] M. Vivero-Lopez, X. Xu, A. Muras, A. Otero, A. Concheiro, S. Gaisford, A.W. Basit, C. Alvarez-Lorenzo, A. Goyanes, Anti-biofilm multi drug-loaded 3D printed hearing aids, Mater. Sci. Eng. C. Mater. Biol. Appl. 119 (2021) 111606, https://doi.org/10.1016/j.msec.2020.111606.
[19] K.P. Iyengar, A.D. Kariya, R. Botchu, V.K. Jain, R. Vaishya, Significant capabilities of SMART sensor technology and their applications for Industry 4.0 in trauma and orthopaedics, Sens. Int 3 (2022) 100163, https://doi.org/10.1016/j.sintl.2022.100163.
[20] N. Ashammakhi, S. Ahadian, F. Zengjie, K. Suthiwanich, F. Lorestani, G. Orive, S. Ostrovidov, A. Khademhosseini, Advances and future perspectives in 4D bioprinting, Biotechnol. J. 13 (2018) e1800148, https://doi.org/10.1002/biot.201800148.
[21] A. Haleem, M. Javaid, R. Vaishya, 5D printing and its expected applications in Orthopaedics, J. Clin. Orthop. Trauma 10 (2019) 809–810, https://doi.org/10.1016/j.jcot.2018.11.014.
[22] S. Anas, M.Y. Khan, M. Rafey, K. Faheem, Concept of 5D printing technology and its applicability in the healthcare industry, Mater. Today Proc. 56 (2022) 1726–1732, https://doi.org/10.1016/j.matpr.2021.10.391.
[23] Cornelius K. Contact lenses are a surprising source of pollution. Scientific American, August 20, 2018. ⟨https://www.scientificamerican.com/article/contact-lenses-are-a-surprising-source-of-pollution/⟩; Accessed August 2023.
[24] A.C. Sousa, A. Veiga, A.C. Maurício, M.A. Lopes, J.D. Santos, B. Neto, Assessment of the environmental impacts of medical devices: a review, Environ. Dev. Sustain. 23 (2021) 9641–9666, https://doi.org/10.1007/s10668-020-01086-1.

[25] FDA. Working Together to Improve Reusable Medical Device Reprocessing. 2022. ⟨https://www.fda.gov/medical-devices/reprocessing-reusable-medical-devices/working-together-improve-reusable-medical-device-reprocessing⟩; Accessed August 2023.
[26] G. Guggenbiller, S. Brooks, O. King, E. Constant, D. Merckle, A.C. Weems, 3D Printing of green and renewable polymeric materials: Toward greener additive manufacturing, ACS Appl. Polym. Mater. 5 (2023) 3201–3229, https://doi.org/10.1021/acsapm.2c02171.
[27] A. Nazir, O. Gokcekaya, K.M. Masum Billah, O. Ertugrul, J. Jiang, J. Sun, S. Hussain, Multi-material additive manufacturing: A systematic review of design, properties, applications, challenges, and 3D printing of materials and cellular metamaterials, Mater. Des. 226 (2023) 111661, https://doi.org/10.1016/j.matdes.2023.111661.
[28] N. Petersen, P. Gatenholm, Bacterial cellulose-based materials and medical devices: current state and perspectives, Appl. Microbiol. Biotechnol. 91 (2011) 1277–1286, https://doi.org/10.1007/s00253-011-3432-y.
[29] L. Dai, T. Cheng, C. Duan, W. Zhao, W. Zhang, X. Zou, J. Aspler, Y. Ni, 3D printing using plant-derived cellulose and its derivatives: a review, Carbohydr. Polym. 203 (2019) 71–86, https://doi.org/10.1016/j.carbpol.2018.09.027.
[30] L. Lin, S. Jiang, J. Yang, J. Qiu, X. Jiao, X. Yue, X. Ke, G. Yang, L. Zhang, Application of 3D-bioprinted nanocellulose and cellulose derivative-based bio-inks in bone and cartilage tissue engineering, Int. J. Bioprint. 9 (2023) 212–229, https://doi.org/10.18063/ijb.v9i1.637.
[31] A. Ji, S. Zhang, S. Bhagia, C.G. Yoo, A.J. Ragauskas, 3D printing of biomass-derived composites: application and characterization approaches, RSC Adv. 10 (2020) 21698–21723, https://doi.org/10.1039/D0RA03620J.
[32] M. Pita-Vilar, A. Concheiro, C. Alvarez-Lorenzo, L. Diaz-Gomez, Recent advances in 3D printed cellulose-based wound dressings: A review on in vitro and in vivo achievements, Carbohydr. Polym. 321 (2023) 121298, https://doi.org/10.1016/j.carbpol.2023.121298.
[33] T. Loftsson, M.E. Brewster, Pharmaceutical applications of cyclodextrins: basic science and product development, J. Pharm. Pharmacol. 62 (2010) 1607–1621, https://doi.org/10.1111/j.2042-7158.2010.01030.x.
[34] N. Morin-Crini, S. Fourmentin, E. Fenyvesi, E. Lichtfouse, G. Torri, M. Fourmentin, G. Crini, 130 years of cyclodextrin discovery for health, food, agriculture, and the industry: a review, Environ. Chem. Lett. 19 (2021) 2581–2617, https://doi.org/10.1007/s10311-020-01156-w.
[35] I. Puskás, L. Szente, L. Szőcs, E. Fenyvesi, Recent list of cyclodextrin-containing drug products, Period. Polytech. Chem. Eng. 67 (2023) 11–17, https://doi.org/10.3311/PPch.21222.
[36] A. Concheiro, C. Alvarez-Lorenzo, Chemically cross-linked and grafted cyclodextrin hydrogels: from nanostructures to drug-eluting medical devices, Adv. Drug Deliv. Revs 65 (2013) 1188–1203, https://doi.org/10.1016/j.addr.2013.04.015.
[37] S.M.N. Simoes, A. Rey-Rico, A. Concheiro, C. Alvarez-Lorenzo, Supramolecular cyclodextrin-based drug nanocarriers, Chem. Comm. 51 (2015) 6275–6289, https://doi.org/10.1039/C4CC10388B.
[38] S.X. Wang, P.J. Ong, S.L. Liu, W. Thitsartam, M.J.B.H. Tan, A. Suwardi, Q. Zhu, X. J. Loh, Recent advances in host-guest supramolecular hydrogels for biomedical applications, Chem. Asian J. 17 (2022) e202200608, https://doi.org/10.1002/asia.202200608.
[39] M. Tang, Z.R. Zhong, C.F. Ke, Advanced supramolecular design for direct ink writing of soft materials, Chem. Soc. Rev. 52 (2023) 1614–1649, https://doi.org/10.1039/D2CS01011A.
[40] A. Cosola, R. Conti, H. Grutzmacher, M. Sangermano, I. Roppolo, C.F. Pirri, A. Chiappone, Multiacrylated cyclodextrin: A bio-derived photocurable macromer for VAT 3D printing, Macromol. Mater. Eng. 305 (2020) 2000350, https://doi.org/10.1002/mame.202000350.
[41] M. Agnes, E. Pancani, M. Malanga, E. Fenyvesi, I. Manet, Implementation of Water-soluble cyclodextrin-based polymers in biomedical applications: How far are we? Macromol. Biosci. 22 (2022) 2200090. ⟨https://doi-org.ezbusc.usc.gal/10.1002/mabi.202200090⟩.
[42] A. Singh, J.A. Zhan, Z.Y. Ye, J.H. Elisseeff, Modular multifunctional poly(ethylene glycol) hydrogels for stem cell differentiation, Adv. Funct. Mater. 23 (2013) 575–582, https://doi.org/10.1002/adfm.201201902.
[43] C. Alvarez-Lorenzo, C.A. García-González, A. Concheiro, Cyclodextrins as versatile building blocks for regenerative medicine, J. Control. Release 268 (2017) 269–281, https://doi.org/10.1016/j.jconrel.2017.10.038.
[44] M. Molnár, E. Fenyvesi, Z. Berkl, I. Németh, I. Fekete-Kertész, R. Márton, E. Vaszita, E. Varga, D. Ujj, L. Szente, Cyclodextrin-mediated quorum quenching in the *Aliivibrio fischeri* bioluminescence model system – Modulation of bacterial communication, Int. J. Pharm. 594 (2021) 120150, https://doi.org/10.1016/j.ijpharm.2020.120150.
[45] G. Brackman, M.J. Garcia-Fernandez, J. Lenoir, L. De Meyer, J.P. Remon, T. De Beer, A. Concheiro, C. Alvarez-Lorenzo, T. Coenye, Dressings loaded with cyclodextrin-hamamelitannin complexes increase *Staphylococcus aureus* susceptibility toward antibiotics both in single as well as in mixed biofilm communities, Macromol. Biosci. 16 (2016) 859–869, https://doi.org/10.1002/mabi.201500437.
[46] M.S. Zhang, W.X. Liu, Q.M. Lin, C.F. Ke, Hierarchically templated synthesis of 3D-printed crosslinked cyclodextrins for lycopene harvesting, Small 19 (2023) 2300323, https://doi.org/10.1002/smll.202300323.
[47] R. Šakalys, K.W. Kho, T.E. Keyes, A reproducible, low cost microfluidic microcavity array SERS platform prepared by soft lithography from a 2 photon 3D printed template, Sens. Actuators B Chem. 340 (2021) 129970, https://doi.org/10.1016/j.snb.2021.129970.
[48] A. González-Campo, S.H. Hsu, L. Puig, J. Huskens, D.N. Reinhoudt, A.H. Velders, Orthogonal covalent and noncovalent functionalization of cyclodextrin-alkyne patterned surfaces, J. Am. Chem. Soc. 132 (2010) 11434–11436. ⟨https://doi-org.ezbusc.usc.gal/10.1021/ja1048658⟩.
[49] D. Ahire, L. Kruger, S. Sharma, V.S. Mettu, A. Basit, B. Prasad, Quantitative proteomics in translational pharmacokinetics, Pharmacol. Revs. 74 (2022) 771–798, https://doi.org/10.1124/pharmrev.121.000449.
[50] I. Seoane-Viaño, P. Januskaite, C. Alvarez-Lorenzo, A.W. Basit, A. Goyanes, Semi-solid extrusion 3D printing in drug delivery and biomedicine: Personalised solutions for healthcare challenges, J. Control. Release 332 (2021) 367–389, https://doi.org/10.1016/j.jconrel.2021.02.027.
[51] J. Conceição, X. Farto-Vaamonde, A. Goyanes, O. Adeoye, A. Concheiro, H. Cabral-Marques, J.M. Sousa Lobo, C. Alvarez-Lorenzo, Hydroxypropyl-β-cyclodextrin-based fast dissolving carbamazepine printlets prepared by semisolid extrusion 3D printing, Carbohydr. Polym. 221 (2019) 55–62, https://doi.org/10.1016/j.carbpol.2019.05.084.
[52] J. Gierbolini, M. Giarratano, S.R. Benbadis, Carbamazepine-related antiepileptic drugs for the treatment of epilepsy - a comparative review, Expert Opin. Pharmacother. 17 (2016) 885–888, https://doi.org/10.1517/14656566.2016.1168399.
[53] H. Wang, L. Hu, L. Peng, J. Du, M. Lan, Y. Cheng, L. Ma, Y. Zhang, Dual encapsulation of β-carotene by β-cyclodextrin and chitosan for 3D printing application, Food Chem. 378 (2022) 132088, https://doi.org/10.1016/j.foodchem.2022.132088.
[54] H. Wang, C. Wu, J. Zhu, Y. Cheng, Y. Yang, S. Qiao, B. Jiao, L. Ma, Y. Fu, H. Chen, H. Dai, Y. Zhang, Stabilization of capsanthin in physically-connected hydrogels: Rheology property, self-recovering performance and syringe/screw-3D printing, Carbohydr. Polym. 319 (2023) 121209, https://doi.org/10.1016/j.carbpol.2023.121209.
[55] E.G. Andriotis, P.K. Monou, A. Louka, E. Papaefstathiou, G.K. Eleftheriadis, D. G. Fatouros, Development of food grade 3D printable ink based on pectin containing cannabidiol/cyclodextrin inclusion complexes, Drug Dev. Ind. Pharm. 46 (2020) 1569–1577, https://doi.org/10.1080/03639045.2020.1791168.
[56] E.G. Andriotis, G.K. Eleftheriadis, C. Karavasili, D.G. Fatouros, Development of bio-active patches based on pectin for the treatment of ulcers and wounds using 3D-bioprinting technology, Pharmaceutics 12 (2020) 56. ⟨https://doi-org.ezbusc.usc.gal/10.3390/pharmaceutics12010056⟩.
[57] S. Li, Y. Jiang, M. Wang, R. Li, J. Dai, J. Yan, W. Qin, Y. Liu, 3D printing of essential oil/β-cyclodextrin/popping candy modified atmosphere packaging for strawberry preservation, Carbohydr. Polym. 297 (2022) 120037, https://doi.org/10.1016/j.carbpol.2022.120037.
[58] J. Thiry, F. Krier, S. Ratwatte, J.M. Thomassin, C. Jerome, B. Evrard, Hot-melt extrusion as a continuous manufacturing process to form ternary cyclodextrin inclusion complexes, Eur. J. Pharm. Sci. 96 (2017) 590–597, https://doi.org/10.1016/j.ejps.2016.09.032.
[59] R.N. Marreto, G. Cardoso, S.B. dos Santos, M. Martin-Pastor, M. Cunha-Filho, S. F. Taveira, A. Concheiro, C. Alvarez-Lorenzo, Hot melt-extrusion improves the properties of cyclodextrin-based poly(pseudo)rotaxanes for transdermal formulation, Int. J. Pharm. 586 (2020) 119510, https://doi.org/10.1016/j.ijpharm.2020.119510.
[60] E. Carlier, S. Marquette, C. Peerboom, K. Amighi, J. Goole, Development of mAb-loaded 3D-printed (FDM) implantable devices based on PLGA, Int. J. Pharm. 597 (2021) 120337, https://doi.org/10.1016/j.ijpharm.2021.120337.
[61] C. Varan, D. Aksut, M. Sen, E. Bilensoy, Design and characterization of carboplatin and paclitaxel loaded PCL filaments for 3D printed controlled release intrauterine implants, Pharmaceutics 15 (2023) 1154, https://doi.org/10.3390/pharmaceutics15041154.
[62] L.D. Cheng, Z.X. Xu, Y.S. Liu, D.Y. Zhou, M. Sun, Y.X. Xu, L.Q. Chen, J. Sun, 3D-Printed drug-loaded composite scaffolds to promote osteogenesis and antibacterial activity, ACS Appl. Polym. Mater. 4 (2022) 4476–4485, https://doi.org/10.1021/acsapm.2c00432.
[63] M. Pistone, G.F. Racaniello, I. Arduino, V. Laquintana, A. Lopalco, A. Cutrignelli, R. Rizzi, M. Franco, A. Lopedota, N. Denora, Direct cyclodextrin-based powder extrusion 3D printing for one-step production of the BCS class II model drug niclosamide, Drug Deliv. Transl. Res. 12 (2022) 1895–1910. ⟨https://doi-org.ezbusc.usc.gal/10.1007/s13346-022-01124-7⟩.
[64] M. Pistone, G.F. Racaniello, R. Rizzi, R.M. Iacobazzi, I. Arduino, A. Lopalco, A. Lopedota, N. Denora, Direct cyclodextrin based powder extrusion 3D printing of budesonide loaded mini-tablets for the treatment of eosinophilic colitis in paediatric patients, Int. J. Pharm. 632 (2023) 122592, https://doi.org/10.1016/j.ijpharm.2023.122592.
[65] G.F. Racaniello, M. Pistone, C. Meazzini, A. Lopedota, I. Arduino, R. Rizzi, A. Lopalco, U.M. Musazzi, F. Cilurzo, N. Denora, 3D printed mucoadhesive orodispersible films manufactured by direct powder extrusion for personalized clobetasol propionate based paediatric therapies, Int. J. Pharm. 643 (2023) 123214, https://doi.org/10.1016/j.ijpharm.2023.123214.
[66] C. Varan, M. Şen, N. Sandler, Y. Aktaş, E. Bilensoy, Mechanical characterization and ex vivo evaluation of anticancer and antiviral drug printed bioadhesive film for the treatment of cervical cancer, Eur. J. Pharm. Sci. 130 (2019) 114–123, https://doi.org/10.1016/j.ejps.2019.01.030.
[67] C. Varan, H. Wickström, N. Sandler, Y. Aktaş, E. Bilensoy, Inkjet printing of antiviral PCL nanoparticles and anticancer cyclodextrin inclusion complexes on bioadhesive film for cervical administration, Int. J. Pharm. 531 (2017) 701–713, https://doi.org/10.1016/j.ijpharm.2017.04.036.
[68] F. Fina, S. Gaisford, A.W. Basit, Powder bed fusion: The working process, current applications and opportunities, in: Basit AW, Gaisford S (Eds.), In 3D printing of

pharmaceuticals, Springer International Publishing, Cham, Switzerland, 2018, pp. 81–105.
[69] N. Allahham, F. Fina, C. Marcuta, L. Kraschew, W. Mohr, S. Gaisford, A.W. Basit, A. Goyanes, Selective laser sintering 3D printing of orally disintegrating printlets containing ondansetron, Pharmaceutics 12 (2020) 110, https://doi.org/10.3390/pharmaceutics12020110.
[70] H.P. Lim, C.O. Karandagaspitiya, D.K.H. Chan, L.E. Low, B.T. Tey, E.S. Chan, Pickering emulsion ink in additive manufacturing: A state-of-the-art review, Addit. Manuf. 73 (2023) 103677, https://doi.org/10.1016/j.addma.2023.103677.
[71] X. Li, L. Fan, R. Li, Y. Han, J. Li, 3D/4d printing of β-cyclodextrin-based high internal phase emulsions, J. Food Eng. 348 (2023) 111455, https://doi.org/10.1016/j.jfoodeng.2023.111455.
[72] X. Li, L. Fan, J. Li, Utilization of polysaccharide-based high internal phase emulsion for nutraceutical encapsulation and 3D printing: Reinforcement of curcumin stability and bioaccessibility, LWT 189 (2023) 115478, https://doi.org/10.1016/j.lwt.2023.115478.
[73] X.Q. Li, L.P. Fan, J.W. Li, Extrusion-based 3D printing of high internal phase emulsions stabilized by co-assembled beta-cyclodextrin and chitosan, Food Hydrocoll. 134 (2023) 108036, https://doi.org/10.1016/j.foodhyd.2022.108036.
[74] S. Li, Y.C. Hao, Q.Y. Gao, Development of emulsion gels stabilized by chitosan and octenyl succinic anhydride-modified β-cyclodextrin complexes for β-carotene digestion and 3D printing, J. Agric. Food Chem. 71 (2023) 18587–18600, https://doi.org/10.1021/acs.jafc.3c05632.
[75] Z. Guo, Z. Li, S. Cen, N. Liang, A. Muhammad, H.E. Tahir, J. Shi, X. Huang, X. Zou, Modulating hydrophilic properties of β-cyclodextrin/carboxymethyl cellulose colloid particles to stabilize Pickering emulsions for food 3D printing, Carbohydr. Polym. 313 (2023) 120764, https://doi.org/10.1016/j.carbpol.2023.120764.
[76] S. Cen, Z. Li, Z. Guo, J. Shi, X. Huang, X. Zou, M. Holmes, Fabrication of Pickering emulsions stabilized by citrus pectin modified with β-cyclodextrin and its application in 3D printing, Carbohydr. Polym. 312 (2023) 120833, https://doi.org/10.1016/j.carbpol.2023.120833.
[77] B. Pang, R. Ajdary, M. Antonietti, O. Rojas, S. Filonenko, Pickering emulgels reinforced with host–guest supramolecular inclusion complexes for high fidelity direct ink writing, Mater. Horiz. 9 (2022) 835–840, https://doi.org/10.1039/D1MH01741A.
[78] T. Higashi, K. Motoyama, H. Arima, Cyclodextrin-based polyrotaxanes and polypseudorotaxanes as drug delivery carriers, J. Drug Deliv. Sci. Technol. 23 (2013) 523–529, https://doi.org/10.1016/S1773-2247(13)50080-3.
[79] A.R. Leonties, A. Baran, G. Ionita, I. Matei, S. Mocanu, R. Baratoiu, E. Hristea, L. Aricov, Physicochemical changes of alginate and polyacrylate mixture induced by interactions of the appended units, Macromol. Chem. Phys. 224 (2023) 2200444, https://doi.org/10.1002/macp.202200444.
[80] Q. Lin, X. Hou, C. Ke, Ring shuttling controls macroscopic motion in a three-dimensional printed polyrotaxane monolith, Angew. Chem. Int. Ed. 56 (2017) 4452, https://doi.org/10.1002/anie.201612440.
[81] M. Mohamadhoseini, Z. Mohamadnia, Supramolecular self-healing materials via host-guest strategy between cyclodextrin and specific types of guest molecules, Coord. Chem. Rev. 432 (2021) 213711, https://doi.org/10.1016/j.ccr.2020.213711.
[82] S.X. Wang, P.J. Ong, S.L. Liu, W. Thitsartam, M.J.B.H. Tan, A. Suwardi, Q. Zhu, X. J. Loh, Recent advances in host-guest supramolecular hydrogels for biomedical applications, Chem. Asian J. 17 (2022) e202200608, https://doi.org/10.1002/asia.202200608.
[83] C. Loebel, C.B. Rodell, M.H. Chen, J.A. Burdick, Shear-thinning and self-healing hydrogels as injectable therapeutics and for 3D-printing, Nat. Protoc. 12 (2017) 1521–1541, https://doi.org/10.1038/nprot.2017.053.
[84] C.B. Rodell, N.N. Dusaj, C.B. Highley, J.A. Burdick, Injectable and cytocompatible tough double-network hydrogels through tandem supramolecular and covalent crosslinking, Adv. Mater. 28 (2016) 8419–8424, https://doi.org/10.1002/adma.201602268.
[85] T. Hu, X. Cui, M. Zhu, M. Wu, Y. Tian, B. Yao, W. Song, Z. Niu, S. Huang, X. Fu, 3D-printable supramolecular hydrogels with shear-thinning property: fabricating strength tunable bioink via dual crosslinking, Bioact. Mater. 5 (2020) 808–818, https://doi.org/10.1016/j.bioactmat.2020.06.001.
[86] S.M.N. Simões, F. Veiga, J.J. Torres-Labandeira, A.C.F. Ribeiro, M.I. Sandez-Macho, A. Concheiro, C. Alvarez-Lorenzo, Syringeable Pluronic-α-cyclodextrin supramolecular gels for sustained delivery of vancomycin, Eur. J. Pharm. Biopharm. 80 (2012) 103–112, https://doi.org/10.1016/j.ejpb.2011.09.017.
[87] Q. Lin, X. Hou, C. Ke, Ring shuttling controls macroscopic motion in a three-dimensional printed polyrotaxane monolith, Angew. Chem. Int. Ed. 56 (2017) 4452, https://doi.org/10.1002/anie.201612440.
[88] E.A. Appel, M.W. Tibbitt, M.J. Webber, B.A. Mattix, O. Veiseh, R. Langer, Self-assembled hydrogels utilizing polymer–nanoparticle interactions, Nat. Commun. 6 (2015) 6295, https://doi.org/10.1038/ncomms7295.
[89] G. Bovone, E.A. Guzzi, S. Bernhard, T. Weber, D. Dranseikiene, M.W. Tibbitt, Supramolecular reinforcement of polymer-nanoparticle hydrogels for modular materials design, Adv. Mater. 34 (2022) 2106941, https://doi.org/10.1002/adma.202106941.
[90] C. Senac, S. Desgranges, C. Contino-Pépin, W. Urbach, P.F.J. Fuchs, N. Taulier, Effect of dimethyl sulfoxide on the binding of 1-adamantane carboxylic acid to β- and γ-cyclodextrins, ACS Omega 3 (2018) 1014–1021, https://doi.org/10.1021/acsomega.7b01212.
[91] C.B. Highley, C.B. Rodell, J.A. Burdick, Direct 3D printing of shear-thinning hydrogels into self-healing hydrogels, Adv. Mater. 27 (2015) 5075–5079, https://doi.org/10.1002/adma.201501234.
[92] L. Ouyang, C.B. Highley, C.B. Rodell, W. Sun, J.A. Burdick, 3D printing of shear-thinning hyaluronic acid hydrogels with secondary cross-linking, ACS Biomater. Sci. Eng. 2 (2016) 1743–1751, https://doi.org/10.1021/acsbiomaterials.6b00158.
[93] C.D. Morley, E.A. Ding, E.M. Carvalho, S. Kumar, A balance between inter- and intra-microgel mechanics governs stem cell viability in injectable dynamic granular hydrogels, Adv. Mater. 35 (2023) 2304212. ⟨https://doi-org.ezbusc.usc.gal/10.1002/adma.202304212⟩.
[94] Z. Wang, G. An, Y. Zhu, X. Liu, Y. Chen, H. Wu, Y. Wang, X. Shi, C. Mao, 3D-printable self-healing and mechanically reinforced hydrogels with host–guest non-covalent interactions integrated into covalently linked networks, Mater. Horiz. 6 (2019) 733–742. ⟨https://doi-org.ezbusc.usc.gal/10.1039/C8MH01208C⟩.
[95] Z. Wang, Y. Ren, Y. Zhu, L. Hao, Y. Chen, G. An, H. Wu, X. Shi, C. Mao, A rapidly self-healing host–guest supramolecular hydrogel with high mechanical strength and excellent biocompatibility, Angew. Chem. Int. Ed. 57 (2018) 9008–9012, https://doi.org/10.1002/anie.201804400.
[96] M. Mohamadhoseini, Z. Mohamadnia, Alginate-based self-healing hydrogels assembled by dual cross-linking strategy: Fabrication and evaluation of mechanical properties, Int. J. Biol. Macromol. 191 (2021) 139–151, https://doi.org/10.1016/j.ijbiomac.2021.09.062.
[97] A.N. Edelbrock, T.D. Clemons, S.M. Chin, J.J.W. Roan, E.P. Bruckner, Z. Álvarez, J.F. Edelbrock, K.S. Wek, S.I. Stupp, Superstructured biomaterials formed by exchange dynamics and host–guest interactions in supramolecular polymers, Adv. Sci. 8 (2021) 2004042 https://doi.org.ezbusc.usc.gal/10.1002/advs.202004042.
[98] K.L. Sampson, B. Deore, A. Go, M.A. Nayak, A. Orth, M. Gallerneault, P.R. L. Malenfant, C. Paquet, Multimaterial vat polymerization additive manufacturing, ACS Appl. Polym. Mater. 3 (2021) 4304–4324, https://doi.org/10.1021/acsapm.1c00262.
[99] L. Rodríguez-Pombo, X. Xu, A. Seijo-Rabina, J.J. Ong, C. Alvarez-Lorenzo, C. Rial, D. Nieto, S. Gaisford, A.W. Basit, A. Goyanes, Volumetric 3D printing for rapid production of medicines, Addit. Manuf. 52 (2022) 102673, https://doi.org/10.1016/j.addma.2022.102673.
[100] X. Xu, A. Awad, P. Robles-Martinez, S. Gaisford, A. Goyanes, A.W. Basit, Vat photopolymerization 3D printing for advanced drug delivery and medical device applications, J. Control. Release 329 (2021) 743–757, https://doi.org/10.1016/j.jconrel.2020.10.008.
[101] L. Pierau, C. Elian, J. Akimoto, Y. Ito, S. Caillol, D.L. Versace, Bio-sourced monomers and cationic photopolymerization–The green combination towards eco-friendly and non-toxic materials, Prog. Polym. Sci. 127 (2022) 101517, https://doi.org/10.1016/j.progpolymsci.2022.101517.
[102] H. Ritter, M. Tabatabai, Cyclodextrin in polymer synthesis: a green way to polymers, Prog. Polym. Sci. 27 (2002) 1713–1720, https://doi.org/10.1016/S0079-6700(02)00022-9.
[103] J. Zhang, F. Dumur, P. Xiao, B. Graff, D. Bardelang, D. Gigmes, J.P. Fouassier, J. Lalevée, Structure design of naphthalimide derivatives: toward versatile photoinitiators for near-UV/visible LEDs, 3D printing, and water-soluble photoinitiating systems, Macromolecules 48 (2015) 2054–2063, https://doi.org/10.1021/acs.macromol.5b00201.
[104] J.F. Xing, J.H. Liu, T.B. Zhang, L. Zhang, M.L. Zheng, X.M. Duan, A water-soluble initiator prepared through host-guest chemical interaction for microfabrication of 3D hydrogels via two-photon polymerization, J. Mat. Chem. B 2 (2014) 4318–4323, https://doi.org/10.1039/C4TB00414K.
[105] M.A. Przybyla, G. Yilmaz, C. Remzi Becer, Natural cyclodextrins and their derivatives for polymer synthesis, Polym. Chem. 11 (2020) 7582–7602, https://doi.org/10.1039/D0PY01464H.
[106] C. Noè, A. Cosola, A. Chiappone, M. Hakkarainen, H. Grützmacher, M. Sangermano, From polysaccharides to UV-curable biorenewable organo/hydrogels for methylene blue removal, Polymer 235 (2021) 124257, https://doi.org/10.1016/j.polymer.2021.124257.
[107] L. Zhang, H. Tang, Z.J. Xiahou, J.H. Zhang, Y.L. She, K.X. Zhang, X.F. Hu, J.B. Yin, C. Chen, Solid multifunctional granular bioink for constructing chondroid basing on stem cell spheroids and chondrocytes, Biofabrication 14 (2022) 035003, https://doi.org/10.1088/1758-5090/ac63ee.
[108] W. Zhao, C. Yue, L. Liu, Y. Liu, J. Leng, Research progress of shape memory polymer and 4D printing in biomedical application, Adv. Healthc. Mater. 12 (2023) 2201975, https://doi.org/10.1002/adhm.202201975.
[109] M. Uboldi, C. Perrotta, C. Moscheni, S. Zecchini, A. Napoli, C. Castiglioni, A. Gazzaniga, A. Melocchi, L. Zema, Insights into the safety and versatility of 4D printed intravesical drug delivery systems, Pharmaceutics 15 (2023) 757, https://doi.org/10.3390/pharmaceutics15030757.
[110] A. Gazzaniga, A. Foppoli, M. Cerea, L. Palugan, M. Cirilli, S. Moutaharrik, A. Melocchi, A. Maroni, Towards 4D printing in pharmaceutics, Int. J. Pharm. X 5 (2023) 100171, https://doi.org/10.1016/j.ijpx.2023.100171.
[111] T. Tang, M. Zhang, A.S. Mujumdar, X. Teng, 3D printed white radish/potato gel with microcapsules: Color/flavor change induced by microwave-infrared heating, Food Res. Int. 158 (2022) 111496, https://doi.org/10.1016/j.foodres.2022.111496.
[112] S. Cen, Z. Li, Z. Guo, H. Li, J. Shi, X. Huang, X. Zou, M. Holmes, 4D printing of a citrus pectin/β-CD Pickering emulsion: A study on temperature induced color transformation, Add. Manuf. 56 (2022) 102925, https://doi.org/10.1016/j.addma.2022.102925.

[113] Q. Lin, L. Li, M. Tang, S. Uenuma, J. Samanta, S. Li, X. Jiang, L. Zou, K. Ito, C. Ke, Kinetic trapping of 3D-printable cyclodextrin-based poly(pseudo)rotaxane networks, Chem 7 (2021) 2442–2459, https://doi.org/10.1016/j.chempr.2021.06.004.
[114] J. Groppi, L. Casimiro, M. Canton, S. Corra, M. Jafari-Nasab, G. Tabacchi, L. Cavallo, M. Baroncini, S. Silvi, E. Fois, A. Credi, Precision molecular threading/dethreading, Angew. Chem. Int. Ed. Engl. 59 (2020) 14825–14834, https://doi.org/10.1002/anie.202003064.
[115] M. Tang, D. Zheng, J. Samanta, E.H.R. Tsai, H. Qiu, J.A. Read, C. Ke, Reinforced double-threaded slide-ring networks for accelerated hydrogel discovery and 3D printing (in press.), Chem (2023), https://doi.org/10.1016/j.chempr.2023.07.020.
[116] J. Mo, S.F. Prevost, L.M. Blowes, M. Egertova, N.J. Terrill, W. Wang, M.R. Elphick, H.S. Gupta, Interfibrillar stiffening of echinoderm mutable collagenous tissue demonstrated at the nanoscale, Proc. Natl. Acad. Sci. USA 113 (2016) e6362–e6371, https://doi.org/10.1073/pnas.160934111.
[117] L. Li, Q. Lin, M. Tang, H.E.R. Tsai, C. Ke, An integrated design of a polypseudorotaxane-based sea cucumber mimic, Angew. Chem. Int. Ed. 60 (2021) 10186–10193, https://doi.org/10.1002/anie.202017019.
[118] R. Xiao, W.M. Huang, Heating/solvent responsive shape-memory polymers for implant biomedical devices in minimally invasive surgery: Current status and challenge, Macromol. Biosci. 20 (2020) 2000108. ⟨https://doi-org.ezbusc.usc.gal/10.1002/mabi.202000108⟩.
[119] Y. Zhou, D. Zhou, P. Cao, X. Zhang, Q. Wang, T. Wang, Z. Li, W. He, J. Ju, Y. Zhang, 4D printing of shape memory vascular stent based on βCD-g-polycaprolactone, Macromol. Rapid Commun. 42 (2021) 2100176, https://doi.org/10.1002/marc.202100176.
[120] W. He, D. Zhou, H. Gu, R. Qu, C. Cui, Y. Zhou, Y. Wang, X. Zhang, Q. Wang, T. Wang, Y. Zhang, A biocompatible 4D printing shape memory polymer as emerging strategy for fabrication of deployable medical devices, Macromol. Rapid Commun. 44 (2023) 2200553, https://doi.org/10.1002/marc.202200553.
[121] T. Shikata, R. Takahashi, Y. Satokawa, Hydration and dynamic behavior of cyclodextrins in aqueous solution, J. Phys. Chem. B 111 (2007) 12239–12247, https://doi.org/10.1021/jp0751864.
[122] H. Kojima, T. Koga, Statistical thermodynamic theory of heat-induced gelation of aqueous methylated polyrotaxane solutions, Macromolecules 49 (2016) 7015–7024, https://doi.org/10.1021/acs.macromol.6b01644.
[123] Q.M. Lin, M. Tang, C.F. Ke, Thermo-responsive 3D-printed polyrotaxane monolith, Polym. Chem. 11 (2020) 304–308. ⟨https://doi-org.ezbusc.usc.gal/10.1039/C9PY01510H⟩.
[124] Q. Lin, L. Li, M. Tang, X. Hou, C. Ke, Rapid macroscale shape morphing of 3D-printed polyrotaxane monoliths amplified from pH-controlled nanoscale ring motions, J. Mater. Chem. C. 6 (2018) 11956–11960, https://doi.org/10.1039/C8TC02834F.
[125] E. Gaidamauskas, E. Norkus, E. Butkus, D.C. Crans, G. Grinciene, Deprotonation of beta-cyclodextrin in alkaline solutions, Carbohydr. Res. 344 (2009) 250–254, https://doi.org/10.1016/j.carres.2008.10.025.
[126] D. Zheng, M. Tang, C.F. Ke, 3D-printed ketoenamine crosslinked polyrotaxane hydrogels and their mechanochromic responsiveness, Polym. Chem. 14 (2023) 2159–2163, https://doi.org/10.1039/D3PY00337J.
[127] B. Healy, T. Yu, D.C. da Silva Alves, C. Okeke, C.B. Breslin, Cyclodextrins as supramolecular recognition systems: applications in the fabrication of electrochemical sensors, Materials 14 (2021) 1668, https://doi.org/10.3390/ma14071668.
[128] X. Xiong, Y. Chen, Z. Wang, H. Liu, M. Le, C. Lin, G. Wu, L. Wang, X. Shi, Y.G. Jia, Y. Zhao, Polymerizable rotaxane hydrogels for three-dimensional printing fabrication of wearable sensors, Nat. Commun. 14 (2023) 1331, https://doi.org/10.1038/s41467-023-36920-3.
[129] J.K. Zhou, H.F. Feng, Q.Q. Sun, Z.K. Xie, X.C. Pang, T. Minari, X.Y. Liu, L. Zhang, Resistance-switchable conjugated polyrotaxane for flexible high-performance RRAMs, Mater. Horiz. 9 (2022) 1526–1535, https://doi.org/10.1039/D1MH01929E.
[130] Q. Wang, X. Ji, X. Liu, Y. Liu, J. Liang, Viscoelastic metal-in-water emulsion gel via host–guest bridging for printed and strain-activated stretchable electrodes, ACS Nano 16 (2022) 12677–12685, https://doi.org/10.1021/acsnano.2c04299.
[131] S. Mohsenifard, S. Mashayekhan, H. Safari, A hybrid cartilage extracellular matrix-based hydrogel/poly(epsilon-caprolactone) scaffold incorporated with Kartogenin for cartilage tissue engineering, J. Biomater. Appl. 37 (2023) 1243–1258, https://doi.org/10.1177/08853282221132987.
[132] X. Zhao, X. Lu, K. Li, S. Song, Z. Luo, C. Zheng, C. Yang, X. Wang, L. Wang, Y. Tang, C. Wang, J. Liu, Double crosslinked biomimetic composite hydrogels containing topographical cues and WAY-316606 induce neural tissue regeneration and functional recovery after spinal cord injury, Bioact. Mater. 24 (2023) 331–345, https://doi.org/10.1016/j.bioactmat.2022.12.024.
[133] S.J. Lee, J.S. Choi, M.R. Eom, H.H. Jo, I.K. Kwon, S.K. Kwon, S.A. Park, Dexamethasone loaded bilayered 3D tubular scaffold reduces restenosis at the anastomotic site of tracheal replacement: in vitro and in vivo assessments, Nanoscale 12 (2020) 4846–4858, https://doi.org/10.1039/C9NR10341D.
[134] Z. Xu, D. Gonzalez-Abradelo, J. Li, C.A. Strassert, B.J. Ravoo, D.S. Guo, Supramolecular color-tunable photoluminescent materials based on a chromophore cascade as security inks with dual encryption, Mater. Chem. Front. 1 (2017) 1847–1852, https://doi.org/10.1039/C7QM00091J.